Formation and Decomposition of Chemically Activated and Stabilized Hydrazine

5 AUTHORS, INCLUDING:

Rubik Asatryan
University at Buffalo, The State University …
51 PUBLICATIONS **366** CITATIONS

SEE PROFILE

Joseph W. Bozzelli
New Jersey Institute of Technology
277 PUBLICATIONS **5,269** CITATIONS

SEE PROFILE

Gabriel da Silva
University of Melbourne
112 PUBLICATIONS **1,767** CITATIONS

SEE PROFILE

Minh Tho Nguyen
University of Leuven
748 PUBLICATIONS **10,846** CITATIONS

SEE PROFILE

Formation and Decomposition of Chemically Activated and Stabilized Hydrazine

Rubik Asatryan,*,† Joseph W. Bozzelli,†,* Gabriel da Silva,‡ Saartje Swinnen,§ and Minh Tho Nguyen§

Department of Chemistry and Environmental Science, New Jersey Institute of Technology, Newark, New Jersey 07102, USA, Department of Chemical and Biomolecular Engineering, The University of Melbourne, Victoria 3010, Australia, and Department of Chemistry, Katholieke Universiteit Leuven, B-3001 Leuven, Belgium

Recombination of two amidogen radicals, NH_2 (X^2B1), is relevant to hydrazine formation, ammonia oxidation and pyrolysis, nitrogen reduction (fixation), and a variety of other N/H/X combustion, environmental, and interstellar processes. We have performed a comprehensive analysis of the N_2H_4 potential energy surface, using a variety of theoretical methods, with thermochemical kinetic analysis and master equation simulations used to treat branching to different product sets in the chemically activated $NH_2 + NH_2$ process. For the first time, iminoammonium ylide (NH_3NH), the less stable isomer of hydrazine, is involved in the kinetic modeling of N_2H_4. A new, low-energy pathway is identified for the formation of NH_3 plus triplet NH, via initial production of NH_3NH followed by singlet−triplet intersystem crossing. This new reaction channel results in the formation of dissociated products at a relatively rapid rate at even moderate temperatures and above. A further novel pathway is described for the decomposition of activated N_2H_4, which eventually leads to the formation of the simple products $N_2 + 2H_2$, via H_2 elimination to *cis*-N_2H_2. This process, termed as "dihydrogen catalysis", may have significant implications in the formation and decomposition chemistry of hydrazine and ammonia in diverse environments. In this mechanism, stereoselective attack of *cis*-N_2H_2 by molecular hydrogen results in decomposition to N_2 with a fairly low barrier. The reverse termolecular reaction leading to the gas-phase formation of *cis*-$N_2H_2 + H_2$ achieves non-heterogeneous catalytic nitrogen fixation with a relatively low activation barrier (77 kcal mol^{-1}), much lower than the 125 kcal mol^{-1} barrier recently reported for bimolecular addition of H_2 to N_2. This termolecular reaction is an entropically disfavored path, but it does describe a new means of activating the notoriously unreactive N_2. We design heterogeneous analogues of this reaction using the model compound $(CH_3)_2FeH_2$ as a source of the H_2 catalyst and apply it to the decomposition of *cis*-diazene. The reaction is seen to proceed via a topologically similar transition state, suggesting that our newly described mechanism is general in nature.

1. Introduction

Hydrazine (N_2H_4) is an important energetic material, the main component of diamine-based rocket fuels. Hydrazine and its methyl-substituted homologues are unique endothermic compounds forming the class of hypergolic propellants. This type of propellant ignites spontaneously on contact with an oxidizer, typically nitrogen tetroxide.[1] N_2H_4 can be stabilized as a flame without any oxidizer, and its decomposition can lead to self-ignition or detonation.[2] Hydrazine, as the simplest diamine, has been the subject of numerous investigations with the earlier literature reviewed comprehensively in refs 3−9.

At adequate pressures, self-reaction of two amidogen radicals generates hydrazine:

$$NH_2 + NH_2 (+M) \rightarrow N_2H_4 (+M) \qquad (1)$$
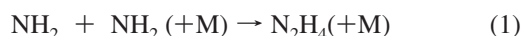
Association and disproportionation reactions involving the NH_2 radical have long been studied experimentally,[4−28] and to a lesser degree by theoretical methods.[29−31]

The N_2H_4 potential energy surface (PES) involves several important transformation pathways closely related to the storage of hydrogen and the fixation of nitrogen (i.e., reduction to NH_3, HCN, etc).[32−35] It is evident that the gas-phase hydrogenation of nitrogen occurs without a catalyst only at extreme conditions, and we note that the degree of this "extremity" and the corresponding energy paths of the process are not well established.
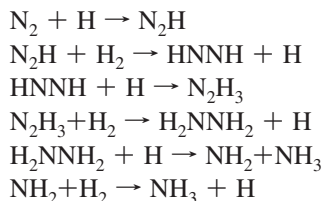
The overall free energy change (ΔG) for the reaction $N_2 + 3H_2 \leftrightarrow 2NH_3$ is about −8 kcal mol^{-1}. However, the first step of activating the triple bond is extremely unfavorable, with bond dissociation energy at 225 kcal mol^{-1}. According to the recent calculations of Hwang and Mebel,[30] the lowest barrier associating H_2 and N_2 into diimide is about 125 kcal mol^{-1} at the G2M(MP2)//MP2/6-31G** level of theory. Such a high activation barrier results in little or no probability for unimolecular occurrence of this reaction in the gas-phase. Hence, chain reactions are considered by the authors as the dominant reaction channels for nitrogen hydrogenation:[30]

* To whom correspondence should be addressed. E-mail: bozzelli@njit.edu (J.W.B.), asatryan@njit.edu (R.A.).
† New Jersey Institute of Technology.
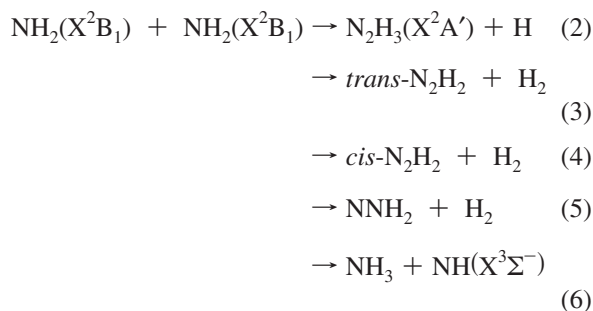‡ University of Melbourne.
§ University of Leuven.

$$N_2 + H \rightarrow N_2H$$
$$N_2H + H_2 \rightarrow HNNH + H$$
$$HNNH + H \rightarrow N_2H_3$$
$$N_2H_3 + H_2 \rightarrow H_2NNH_2 + H$$
$$H_2NNH_2 + H \rightarrow NH_2 + NH_3$$
$$NH_2 + H_2 \rightarrow NH_3 + H$$

$$\text{Net: } N_2 + 3H_2 \rightarrow 2NH_3$$

Recent studies substantiate that N_2H_4 is an intermediate reaction product in the thermal decomposition of ammonia (at 800 °C).[38] Chain-mediated decomposition of hydrazine is known from classic literature: $2N_2H_4 \rightarrow 2NH_3 + N_2 + H_2$ with chain steps $N_2H_4 \rightarrow H + N_2H_3 \rightarrow H + N_2H_2 \rightarrow N_2 + H_2$.[4]

There are a number of unresolved problems in the mechanism of nitrogen fixation in biological media (reduction of N_2 to NH_3 by nitrogenase via bacterial enzymes, nitrogen metabolism in archaea, etc.).[33] Notably, hydrogen is always produced when nitrogenase reduces N_2 to NH_3 (vide infra). Most N_2 fixing bacteria contain hydrogenase to recycle hydrogen.[34] There is an agreement that N_2 binds end-on to the Fe[H]$_2$ complex and releases H_2, while the bound N_2 is reduced to N_2H_2. Hydrazine as an intermediate has been detected experimentally whereas N_2H_2 is assumed to be a very unstable intermediate that tends to decompose back to $N_2 + H_2$.[33]

It is also believed that the primary initiation step in the thermal de-NO$_x$ processes is the reaction of ammonia with hydroxyl to form amidogen (NH_2).[6,36] The temperature dependence of the thermal de-NO$_x$ process depends on the behavior of NH_2. Recombination and cross-reactions of NH_2 radicals with simple open and closed-shell species such as O_2, NO, O_3, SO_2, and CO, along with the oxidation of NH_3, are also of principal importance in combustion media, environmental processes, and in atmospheric chemistry.[28,37]

The amidogen radical self-reaction involves several disproportionation channels

$$NH_2(X^2B_1) + NH_2(X^2B_1) \rightarrow N_2H_3(X^2A') + H \quad (2)$$
$$\rightarrow trans\text{-}N_2H_2 + H_2 \quad (3)$$
$$\rightarrow cis\text{-}N_2H_2 + H_2 \quad (4)$$
$$\rightarrow NNH_2 + H_2 \quad (5)$$
$$\rightarrow NH_3 + NH(X^3\Sigma^-) \quad (6)$$

The association reaction has been implicated as an important reaction in rich ammonia flames.[10] The nitrogen chemistry mechanism of Dean and Bozzelli,[6] as well as Konnov's recent N/H mechanism[8] based on an earlier review of Hanson and Salimian,[5] include most of these reaction systems governing decomposition of hydrazine and controlling the propagation speed of the hydrazine flame. Despite the fundamental importance of this system, the detailed mechanism remains incomplete and unclear. Several of these key reactions do not have accurate and certain kinetic parameters, and, it appears, some mechanisms and rate parameters are controversial. We also believe some principal reaction channels are missing (vide infra).

Due to the difficulties in mass-spectrometric differentiation of diazene isomers relevant to the reactions 3−5, no distinction

is made in some kinetic models between isomers of N_2H_2 and they are often combined into one reaction by use of a single average N_2H_2 species. Analysis of the principal energetic, structural, and kinetic differences between *trans*-N_2H_2, *cis*-N_2H_2, and NNH_2 (also called *iso*-N_2H_2) show significant distinctions. Kinetic analysis in this study suggests that the specific isomer that forms or dominates in a given process may well play a crucial role in the final integrated results. Dean et al. proposed[10] that the recombination reaction $NH_2 + NH_2$ had two channels to $N_2H_3 + H$ and N_2H_4 to better explain their radical profile measurements in rich ammonia flames. Formation of an N_2H_4 product appears to dominate at lower-temperatures in agreement with literature data[8] with wide variation in the reported rate constants. Other reaction channels, however, are less consistent. Miller and Bowman suggested[7] that the high-temperature products are $N_2H_2 + H_2$. The measurements by Stothard et al.[25] at room temperature and low pressures indicate that H_2 production is the dominant channel. They deduced a rate coefficient for the bimolecular channel of amidogen recombination forming N_2H_2 as 7.8×10^{11} cm^3 mol^{-1} s^{-1}. However, the mass-spectrometric method used by these authors did not allow for assigning an observed experimental value to one of the N_2H_2 coproduct isomers. Dean and Bozzelli have further examined this system[6] to try to account for the observations of Stothard et al.[25] at ambient temperatures and have interpreted their results in terms of a new reaction channel to H_2 and singlet H_2NN. To account for reactions of H_2NN in nitrogen mechanisms, several rate constants for a series of related reactions have been proposed.[6] Recent modeling of Konnov and De Ruyck[8] demonstrates that reactions forming N_2H_2, as well as their unimolecular decomposition and bimolecular radical reactions, are important in hydrazine flames, since N_2H_2 is a crucial intermediate.
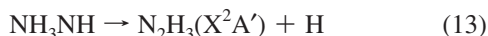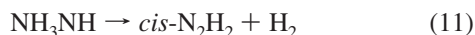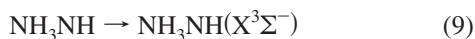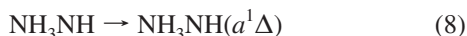
Decomposition of gaseous hydrazine behind a reflected shock wave is found to be pressure dependent; the falloff behavior depends on the nature of diluents.[27] The main products of hydrazine decomposition are ammonia, hydrogen, and nitrogen. Relative yields of the products in hydrazine decomposition flames closely correspond to the overall equation $2N_2H_4 \rightarrow 2NH_3 + N_2 + H_2$, and their relative yields were found to be unaffected by pressure.[11,39] Notably, less ammonia is formed in hydrazine decomposition at higher temperatures.[40] An inclusive review on the kinetic modeling of decomposition of hydrazine using different estimated rate constants is contained in the Konnov and De Ruyck article,[8] while some early models are described by Adams.[41]

The overall recombination process of amidogen radicals have been considered quite recently by Bahng and Macdonald[28] at 293 ± 2 K over a pressure range from 2 to 10 Torr. The low pressure rate constant showed a linear dependence on pressure. The sum of the disproportionation rate constants (the zero pressure rate constant) is estimated as $(3.4 \pm 6) \times 10^{-13}$ cm^{-3} molecule^{-1} s^{-1}.

A detailed theoretical study concerning the transformations of N_2H_4 was recently reported by Hwang and Mebel, while studying the hydrogenation of nitrogen, $N_2 + 3H_2 \rightarrow 2NH_3$, employing G2M(MP2) composite method on geometries optimized at MP2/6-31G(d,p) ab initio level.[30] Three transition states leading to the formation of molecular hydrogen accompanied by the formation of *cis*-N_2H_2, *trans*-N_2H_2, and NNH_2 isomers were identified. These paths, however, have very high barriers of activation respective to the $NH_2 + NH_2$ recombination channel. The substantial barrier for formation of the *cis*-N_2H_2 isomer of diazene is in agreement with earlier calculations.[6] On

Kinetic Analysis of the NH₂ + NH₂ Reaction

J. Phys. Chem. A, Vol. 114, No. 21, 2010 **6237**

the other hand, the NNH$_2$ formation kinetics was found to be significantly less favorable. Hence, the question of the existence of a unimolecular pathway(s) for low-temperature formation of diazene observed experimentally remains open (recalling that dominant formation of hydrogen at lower temperatures is claimed by Stothard an co-workers using mass-spectrometry data).[25] Perhaps, due to the specific goal of Hwang and Mebel[30] to locate primary hydrogenation channels to NH$_3$, some specific pathways related to hydrazine (as will be discussed below) were not revealed in their study. Particularly, the anti-isomer of hydrazine is the only one considered by these authors, where the gauche-isomer is a global minimum on the PES.

In the present work, we have performed a systematic and comprehensive ab initio and density functional theory (DFT) study and kinetic analysis of the NH$_2$ + NH$_2$ reaction, including decomposition pathways of activated and stabilized hydrazine, to explore in detail the reaction mechanism and to evaluate corresponding kinetic parameters. Along with the corrections made in some rate parameters for traditional pathways, we have also revealed several new pathways involving the less stable and lesser known isomer of hydrazine,[3] iminoammonium ylide, NH$_3$NH:

$$N_2H_4 \rightarrow NH_3NH \qquad (7)$$

$$NH_3NH \rightarrow NH_3NH(a^1\Delta) \qquad (8)$$

$$NH_3NH \rightarrow NH_3NH(X^3\Sigma^-) \qquad (9)$$

$$NH_3NH \rightarrow trans\text{-}N_2H_2 + H_2 \qquad (10)$$

$$NH_3NH \rightarrow cis\text{-}N_2H_2 + H_2 \qquad (11)$$

$$NH_3NH \rightarrow NNH_2 + H_2 \qquad (12)$$

$$NH_3NH \rightarrow N_2H_3(X^2A') + H \qquad (13)$$

Reaction 8 leads to the iminoammonium isomer with dissociation limit of 47.0 kcal mol^{-1} evaluated at the CCSD(T)/aug-cc-pVTZ level, in agreement with the product enthalpy evaluations in the literature (Table 1). Reaction 9, on the other hand, is spin-forbidden and can proceed only via intersystem crossing between singlet and triplet electronic states, as is shown below.

We also reveal a new stereoselective reaction channel for the formation of simple elementary products with fairly low activation barrier (see Section 5 for details):

$$cis\text{-}N_2H_2 + H_2 \rightarrow N_2 + H_2 + H_2 \qquad (14)$$

We discuss thoroughly the formation of *cis*-N$_2$H$_2$ as an important intermediate in the overall decomposition mechanism of hydrazine.

2. Computational Methods

2.1. Electronic Structure and Energetics. The thermochemistry, reaction paths, and kinetics for decomposition of hydrazine have been investigated with a variety of composite and single-level ab initio (wave function theory) and DFT

methods, as implemented in the Gaussian 03[42] and Molpro[43] suites of programs. Stationary points on the PES of interest were first localized at B3LYP density functional level using 6-31G(d,p) and extended to 6-311++G(3df,3dp) basis sets. This hybrid functional is a widely tested method and is considered accurate for frequency and structural parameters.[44] To confirm the validity of B3LYP geometries we have also performed MP2/6-311++G(3df,3dp) ab initio level calculations.[44]

To improve energetics of the PES we recalculated stationary points at higher levels using the CBS-QB3, CBS-APNO, and W1 composite methods, along with different level individual ab initio methods including coupled cluster singles and doubles with perturbative triples CCSD(T) and related quadratic configuration interaction QCISD(T) methods in conjunction with the different basis sets. CBS-QB3 and CBS-APNO composite methods are both multilevel protocols for the calculation of molecular energies designed by Peterson's group.[45] We also used W1 theory, which is a benchmark method for some systems, for comparison.[46] Composite theoretical protocols are popular well-tested methods for nitrogen chemistry as shown for example in some of our previous work,[47,48] particularly using CBS-QB3 theory.

All reported transition states are characterized as having only one negative eigenvalue of Hessian (force constant) matrices. The absence of imaginary frequencies verifies that species structures are true minima at their respective levels of theory. The intrinsic reaction coordinate (IRC) procedure is used to identify the connectivity of stationary points on the respective PES cross sections. The final IRC scan points are further optimized to ensure that reaction from each saddle point leads to the proper reactants and products.

Spin contamination of the open-shell systems in this study was small as judged by the corresponding $\langle S^2 \rangle$ expectation values. In unrestricted B3LYP calculations $\langle S^2 \rangle$ values for radicals were less than 0.76 before and 0.75 after spin annihilation. For the transition states $\langle S^2 \rangle$ was larger (ca. 0.84); however, all values of $\langle S^2 \rangle$ were ≤0.755 after spin annihilation. Spin contamination in composite methods was also small ($\langle S^2 \rangle$ less than 0.78). Expectation values were ≤2.05 for triplet species.

To avoid spin contamination in some species, specifically NH($^1\Delta$) and TS1, a restricted CCSD(T) analysis is preferred over an unrestricted wave function. Consider the singlet imidogen, ^{1}NH, for instance, expectation values calculated within a number of noncomposite methods B3LYP, MP2, CCSD, CCSD(T), QCISD(T), vide infra, appears to be rather high ($\langle S^2 \rangle \approx 1$) before annihilation. Consequently, the S → T splitting energy with ^{3}NH is predicted to be anomalously low (~10 to 19 kcal mol^{-1} instead of 35–40 kcal mol^{-1}, vide infra) while using these methods. Corresponding spin restricted methods were applied giving correct energetics. Results in comparison with the available experiments are presented in Tables 1 and 2. Note also that the calculated values are correct while calculating molecular complexes involving NH fragment as a part of united system (supermolecule calculation), e.g., while scanning the N−N bond in an iminoammonium ylide, NH$_3$NH, leading to the formation of singlet ^{1}NH and NH$_3$ product set. Apparently, this arises due to switching to the restricted wave function option in the "supermolecule" calculations.

The single determinant nature of wave functions for all calculated structures was tested by calculation of T1 diagnostics parameters.[49] The T1 parameters of key transition states and local minima were found to be small (0.02−0.04). The exception is T1$_{TS1}$ = 0.18; this system is the subject of special attention below.
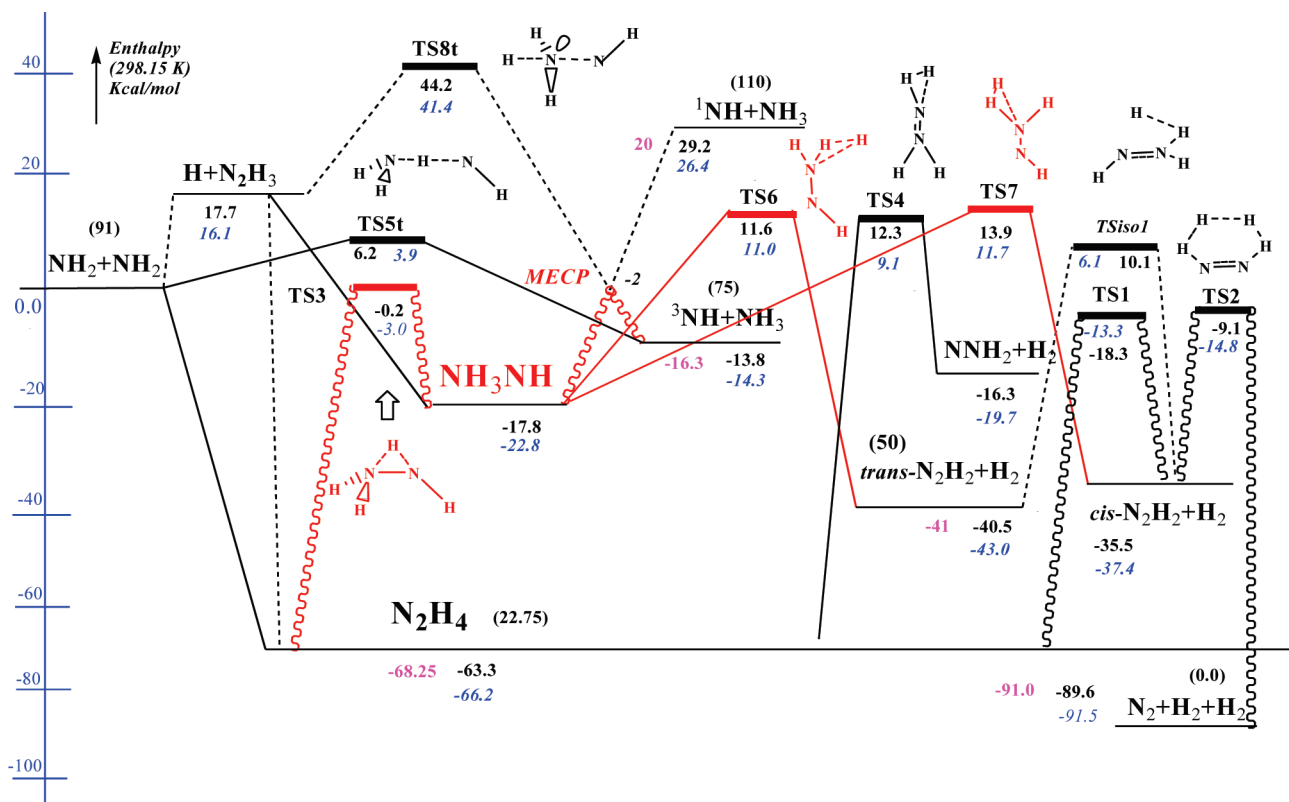
Figure 1. Selected cross sections on the PES of hydrazine, N_2H_4, calculated at CCSD(T)/CBS + ZPE (CCSD(T)/aug-pVTZ) level of theory. CBS-QB3 enthalpies at 298 K are in italics, for comparison. Experimental data are in pink; experimental formation enthalpy values at 298 K are in parentheses. TS1 sets at CBS-QB3 value (see text for explanation). PE diagram involves singlet surface reactions as well as two bimolecular reactions on triplet surface (via TS5t and TS8t) leading to the formation of triplet imidogen radical. MECP indicates the minimal energy crossing point from the QCISD/6-311+G(3df,2p) level calculations. Reactions involving NH_3NH isomer are highlighted in red. Toothed (saw-like) lines indicate lowest pathways to product sets $^3NH + NH_3$ (via MECP) and $N_2 + 2H_2$ (via TS1−TS2).

It should be emphasized that the composite method CBS-QB3 has a correction parameter for spin contaminated systems, which may appear essential in predicting the energetics of the most questionable transition state, TS1 leading to the unimolecular formation of *cis*-N_2H_2 (vide supra).

All values presented in this work are for a standard state of 298.15 K and 1 atm unless otherwise stated.

2.2. Calculation of Kinetic Parameters. Quantum Rice−Ramsperger−Kassel (QRRK) analysis is used to calculate $k(E)$ for each reaction intermediate to respective isomers and product channels. Master equation analysis is used to determine falloff and collisional stabilization. Vibrational frequencies and moments of inertia are taken from DFT calculations. Rate constants for elementary reactions are calculated using classical transition state theory (TST).[44a]

High-pressure limit rate constants are obtained by fitting TST values at 300−2000 K to the three-parameter modified Arrhenius equation, $k^\infty = AT^n \exp(-E/RT)$, where A, n, E are the corresponding rate constant parameters. Required input information for the three-frequency (reduced frequency set) QRRK model[50] is calculated using standard procedures implemented in the SMCPS[51] and THERM[52] codes.

3. Results and Discussion

Selected cross sections on the N_2H_4 PES, calculated at the CCSD(T)/CBS + ZPE (CCSD(T)/aug-cc-pVTZ) level of theory are presented in Figure 1, with the entrance channel corresponding to the recombination of two amidogen NH_2 radicals. CBS-QB3 enthalpies at 298 K (blue italics in Figure 1) are also

presented for comparison. Table 1 contains evaluated enthalpies while Table 2 contains relative energies at different levels of theory.

The potential energy diagram involves singlet surface reactions along with the two bimolecular reactions on the triplet surface (via TS5t and TS8t) leading to formation of the ground state triplet imidogen radical, NH(X$^3\Sigma^-$). Several of the PES cross sections are of primary interest and will be discussed below in detail.

3.1. Thermochemistry of Species and Justification of Methods. Calculated thermochemical parameters ($\Delta_fH^\circ_{298}$, S°, C_p) for species involved in the N_2H_4 energy surface along with the limited experimental and literature values are presented in Tables 1 and 4.

Enthalpy calculations at 298 K have been mainly performed using simplified atomization procedure.[47] As we demonstrated previously,[47,48] composite methods, especially CBS-QB3, perform well in predicting the thermochemical properties of nitrogen containing compounds. More broadly, the CBS-QB3 method provides a mean absolute deviation of 0.9 kcal mol^{-1} for all experimental energies in the G2 test set.[45]

The results listed in Table 1 are in good agreement with the available literature values. The well-depth for the $NH_2 + NH_2$ association reaction, calculated using experimental enthalpies for NH_2 and N_2H_4, is 68.25 kcal mol^{-1}. The predicted value of 66.3 kcal mol^{-1} at the CBS-QB3 level appears to be the closest one among the theoretical data (see Figure 1 and Table 2). The singlet−triplet splitting energy in the imidogen radical is calculated as 40.7 and 42.0 kcal mol^{-1} at the CBS-QB3 and

Kinetic Analysis of the NH$_2$ + NH$_2$ Reaction

J. Phys. Chem. A, Vol. 114, No. 21, 2010 **6239**

TABLE 1: Calculated and Experimental Formation Enthalpies ($\Delta_f H^\circ_{298}$) for Species Involved in the Potential Energy Surface of N$_2$H$_4$

species	CBS-QB3	CBS-APNO	B3LYP/6-311+G(3df,2p)	expt.	lit. calc.
^{1}NH	126.93	128.58	96.16	122.0[a], 121.8[b]	
^{3}NH	86.28	86.22	82.52	90 ± 4[c]; 85.67 ± 2.39[d]	85.94[e]
NH$_2$	45.04	44.95	42.55	45.5 ± 1.51[f]	44.58[e]
NH$_3$	−10.47	−10.78	−9.12	−10.98 ± 0.08[g]	
trans-N$_2$H$_2$	48.17		47.23	50.64[d]	46.94[h]
cis-N$_2$H$_2$	53.31		52.53		52.27[h]
NNH$_2$	71.53		68.52		68.93[h]
N$_2$H$_3$	54.10		48.94		53.7[l], 55.3[h]
gauche-N$_2$H$_4$	23.84	24.03	23.18	22.75[j]	
NH$_3$NH	67.19	67.69	70.72		

[a] Based on vacuum-ultraviolet photolysis of N$_2$H$_2$; ref 74 [b] Sandia compilations; ref 56. [c] At 0 K; ref 53. [d] Ref 58. [e] Ref 59. [f] Ref 71. [g] Ref 70. [h] BAC-MP4 value; Ref 54. [l] CCSD(T) value; Ref 55. [j] Ref 58.

TABLE 2: Calculated at Different Levels of Theory Relative Energies (in kcal mol^{-1}) for Species Involved in the Potential Energy Surface of Hydrazine, N$_2$H$_4$

| Species	CBS-QB3	CCSD(T)[a]//CBS-QB3	QCISD(T)[b]//CBS-QB3	CCSD(T)[c]/CBS	B3LYP[d]	MP2[d]	B97−1[h]	Expt.[l]
NH$_2$ + NH$_2$	0	0	0	0	0	0	0	0
N$_2$H$_4$	−66.3	−62.33	−62.57	−63.3	−61.93	−65.31	−65.51	−68.25
NH$_3$NH	−22.81	−17.92	−18.31	−17.8	−14.40	−14.6	−22.5	
N$_2$H$_3$ + H	16.12	17.85	17.45	17.7	15.93	13.28	12.1	
NH$_3$ + ^{a}NH	26.37	29.65	29.59	29.2	41.45	400.67	37.3	∼20
NH$_3$ + ^{c}NH	−14.27	−14.62	−14.71	−13.8	−11.71	−17.52	−12.1	−16.3
N$_2$H$_2$-*trans* + H$_2$	−43.04	−39.65	−39.95	−40.5	−39.88	−45.27	−38.1	−41
N$_2$H$_2$-*cis* + H$_2$	−37.41[e]	−34.36	−34.75	−35.5	−33.27	−39.38	−33.0	
NNH$_2$ + H$_2$	−19.68	−15.49	−15.33	−16.3	−18.60	−16.28	−16.9	
N$_2$ + H$_2$ + H$_2$	−91.55	−88.74	−89.29	−89.6	−83.38	101.55	−79.6	−91.0
TS1	−13.32	−18.27	34.38		15.4	30(49)[f]	43.8	
TS2	−14.82	−10.70	−10.88	−9.1	−16.90	−19.04	−15.0	
TS3	−3.04	1.23	0.95	−0.2	1.51	3.05	−3.3	
TS4	9.14	13.15	12.83	12.3	6.83	15.3	6.2	
TS5t	3.91	5.21	4.99	6.2	−1.71	7.5	−1.1	
TS6	10.95	14.95	14.92	11.6	14.88	18.16	14.0	
TS7	11.65	15.61	15.33	13.9	15.34	18.95	14.4	
TS8t	41.38	43.55	43.21	44.2	37.35	47.75	39.3	
MECP[g]			−2					

[a] CCSD(T)/6-311+G(2df,2p) at CBS-QB3 geometries. [b] Using 6-311+G(2df,2p) basis set; minima at QCISD and transition states at CBS-QB3 geometries. [c] At CCSD(T)/CBS + ZPE(CCSD(T)/aug-cc-pVTZ) level. [d] Using 6-311++G(3df,3dp) basis set. [e] Respective to the *vdw* complex; calculated value in respect to the isolated system is −34.90 kcal mol^{-1}. [f] Different TS structures leading to the same products, see text. [g] Minimal energy crossing point. [h] Using correlation consistent aug-cc-pVTZ basis set. [l] See Table 1.

CCSD(T)/CBS levels versus an experimental value of 36.28 kcal mol^{-1}.[75]

Another parameter that is easily compared to experiment is the N−H bond dissociation energy in hydrazine to the N$_2$H$_3$ and H radicals, where the experimental value from Ruscic and co-workers is 80.08 kcal mol^{-1}.[53] Results derived from data in Table 2 almost coincide with this value, both at CCSDT(T)/aug-cc-pVTZ/CBS and CCSDT(T)/6-311+G(3df,2p)//CBS-QB3 levels: 80.00 and 80.18 kcal mol^{-1}, correspondingly.

3.2. Direct Hydrogen Abstraction Reaction via TS5t. Interaction of two amidogen radicals leads to direct disproportionation to NH$_3$ and imidogen (NH):

$$NH_2 + NH_2 \rightarrow NH_3 + NH \qquad (6)$$
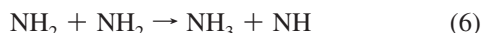
This reaction is routinely considered as the major channel for the formation of imidogen in N/H systems. The main concern here is the electronic state of the formed imidogen radical and the possible correlation to the triplet spin manifold.

This reaction channel is exothermic ($\Delta_r H^\circ_{298} = -16$ kcal mol^{-1}) for ground state NH, which is known to be a triplet (X$^3\Sigma^-$), (cf. Table 1).

As seen from Figure 1, this reaction proceeds on the triplet surface surmounting the transition state TS5t. The barrier height for this collinear reaction varies from 3 to 6 kcal mol^{-1} depending on the method used (see Table 2). The barrier at the MP2 level, for example, is obtained as 3.73 kcal mol^{-1}, which is in agreement with a literature value evaluated at the same level using however a smaller basis set.[29]

The high temperature rate constant as determined by Davidson et al.[24] from 2000−2800 K is 5.0×10^{13} exp($-10\,000/RT$) cm^3 mol^{-1} s^{-1} and is ascribed to the H-atom abstraction process discussed here.

Imidogen is formed from decomposition of chemically activated NH$_3$NH, as is seen from Figure 1. This process proceeds on the singlet surface with a substantial energy gain. The dissociation limit for iminoammonium ylide to form singlet NH($a^1\Delta$) is predicted to be 47.57, 47.8, and 49.2 kcal mol^{-1} at CCSD(T), QCISD(T), and CBS-QB3 levels, respectively.

Calculation on singlet imidogen encountered severe spin contamination, leading to incorrect results when using unrestricted wave functions and single level methods. Expectation values for the spin operator calculated at the B3LYP/6-311++G(3df,3dp), MWKB1K/6-31G(d,p), TPSSLYP1W/6-31G(d,p) DFT and MP2/6-311++G(3df,3dp), CCSD/6-

311+G(2df,2p), CCSD(T)/6-311+ G(2df,2p) and QCISD(T)/6-311+G(2df,2p) ab initio levels appear to be rather high ($\langle S^2 \rangle \approx 1$ before annihilation). As a consequence, predicted S → T splitting energies are anomalously low (~10 to 19 kcal mol^{-1} vs correct value of 35−40 kcal mol^{-1}, vide infra). To avoid spin contamination in NH($a^1\Delta$), restricted wave function analysis is preferred over unrestricted ones. Employment of spin restricted methods lead to the reasonable energetic values as seen in Table 2.

We note that composite methods appear to predict correct values for imidogen due to the use of restricted wave functions. By the same reasoning, all individual methods, including those failing to calculate ^{1}NH−^{3}NH splitting, give reasonable results while using a "super-molecular" approach, for example, calculation of dissociation limits in a *"molecular complex"* involving the fragment of interest such as NH···NH$_3$, employing the restricted wave function options.

Several individual methods predict transition states (considered as nonvalid) for bimolecular reactions (singlet TS5) with energy below the entrance channel, as a result of the large spin contamination in singlet imidogen. In contrast, all the methods considered here predict valid transition states to the formation of NH ($X^3\Sigma^-$) via TS5t when this process proceeds on the triplet surface; this is in agreement with the available theoretical data.[29,30]

3.3. Tautomerization of Hydrazine (eq 7). Figure 1 shows a feasible pathway to the unimolecular tautomerization of (energized) hydrazine into iminoammonium ylide, NH$_3$NH, via transition state TS3. This is a normal N−N bond isomerization to a highly polar product with zwitterionic N−N bond character. The sum of effective Mulliken atomic charges on two opposite groups of NH$_3$NH calculated at QCISD(T)/6-311+(2df,2p) level are Q(NH) = −0.4e and Q(NH$_3$) = +0.4e, resulting in a high dipole moment for this molecule, $\mu = 5.5$ D.

NH$_3$NH is a less known isomer of hydrazine initially introduced in our previous work[3] on the kinetic modeling of N$_2$H$_4$, and to our knowledge it has not yet been observed experimentally. The NH$_3$NH structure was, however, recently considered to exist in intercalates of the kaolinite clay based on IR spectroscopic analysis.[60]

Theoretically this NH$_3$NH molecule along with its isoelectronic and heteroatom analogues was studied first by Pople et al.,[61] then by Pamidighantam and Lammertsma, both at the MP2 level.[62] It was analyzed in more detail recently by Ding and Zhang,[63] Skurski et al.,[64] and Hwang and Mebel.[30] Note that all literature structure calculations have been performed using MP2 based Hamiltonians except for the bound electron calculations performed by Skurski et al.[64] at the coupled cluster CCSD(T) level. Despite the apparent importance of this isomer, corresponding reactions have not yet been included in kinetic models.[3]

As seen in Figure 1 and Table 2, exothermic isomerization of iminoammonium ylide to N$_2$H$_4$ (TS3) has a barrier of 19.15, 19.2, and 19.7 kcal mol^{-1}, correspondingly at CCSD(T), CBS-QB3, and QCISD(T) levels. These values compare well with the literature values indicated above, which are all around 19.5 kcal mol^{-1}.[29,30] The reverse reaction to NH$_3$NH is endothermic by ca. 44 kcal mol^{-1} (44.41, 44.20, and 43.5 kcal mol^{-1}, respectively), and has a barrier of ca. 63 kcal mol^{-1} (63.5, 63.4, and 63.2 kcal mol^{-1}, respectively). It should be emphasized that all results for this N$_2$H$_4 \leftrightarrow$ NH$_3$NH transformation reaction are in excellent agreement with each other.

3.4. Intersystem Crossing: Minimum Energy Crossing Point (MECP) with Dissociation of NH$_3$NH. As indicated above, unimolecular decomposition of chemically activated NH$_3$NH on a singlet surface is not feasible. The dissociation limit (eq 8) at the CCSD(T) level forming singlet NH is 47.5 kcal mol^{-1}.

$$NH_3NH \rightarrow NH_3 + NH(a^1\Delta) \qquad (8)$$

The ground state of NH is known to have triplet NH($X^3\Sigma^-$) electronic state and hence reaction 9 is spin-forbidden

$$NH_3NH \rightarrow NH_3 + NH(X^3\Sigma^-) \qquad (9)$$

Reaction 9 could serve as an important channel, however, if it happens to cross with its singlet counterpart: a relevant electronic term of another pathway leading to the same set of products. In an effort to predict alternative channels to produce ground triplet state imidogen, NH ($X^3\Sigma^-$) we have studied the vicinity of spin-forbidden reaction 9 assuming that there would be a region for a low-lying exited state to cross with a relevant ground state electronic term.

We have outlined two structurally close regions where singlet−triplet crossing is potentially possible. The first one is located in the vicinity of TS3 (the "hop" to the topologically close TS5t), and another one appears to be the interconnection of the dissociation curve of NH$_3$NH and the bimolecular reaction of H + N$_2$H$_3$, which leads to the analogous set of products (indicated as MECP on the toothed line in Figure 1, vide infra).

Formation of triplet imidogen on the triplet surface through reaction of H + N$_2$H$_3$ proceeds via direct replacement (push-out) of the NH group by an approaching H atom passing through a trigonal bipyramidal transition state (TS8t). The process is quite similar to the Walden inversion mechanism in S$_N$2 type reactions (Figure 2). As was expected, the barrier for the exchange of H with the NH group caused by inversion of the nitrogen center is rather high, ca. 43 kcal mol^{-1} (Table 2). Hence, the rate of direct reaction should be low even at elevated temperatures. This reaction may, however, play an important role due to switching to the monomolecular decomposition channel (eq 8) for NH$_3$NH intermediate, which leads to the highly energetic singlet imidogen radical NH($a^1\Delta$) and NH$_3$.

The minimal energy crossing point (MECP) has been localized using QCISD(T) ab initio method and B3LYP hybrid DFT, for comparison. The results are fairly close to each other. Figure 2 represents only results at the QCISD(T)/6-311++G(3df,3dp) level with the optimization of all internal geometry parameters.

The developed pathway suggests a new, feasible channel to the decomposition of NH$_3$NH isomer into the ground state (triplet) imidogen and ammonia through a chemically activated mechanism with intersystem crossing of iminoammonium ylide. Note that rate parameters for such an intersystem crossing will obviously depend on the effectiveness of crossing and quenching parameters not addressed here.

3.5. Bond Dissociation and Isomerization of Intermediate Species. Here we address two isomers of hydrazine, the N$_2$H$_3$ intermediate radical and the three main isomers of N$_2$H$_2$ directly involved in pathways shown in Figure 1. Dissociation of hydrazine-related smaller particles such as N$_2$H and NH possibly form in chain reactions and are beyond the scope of this work;
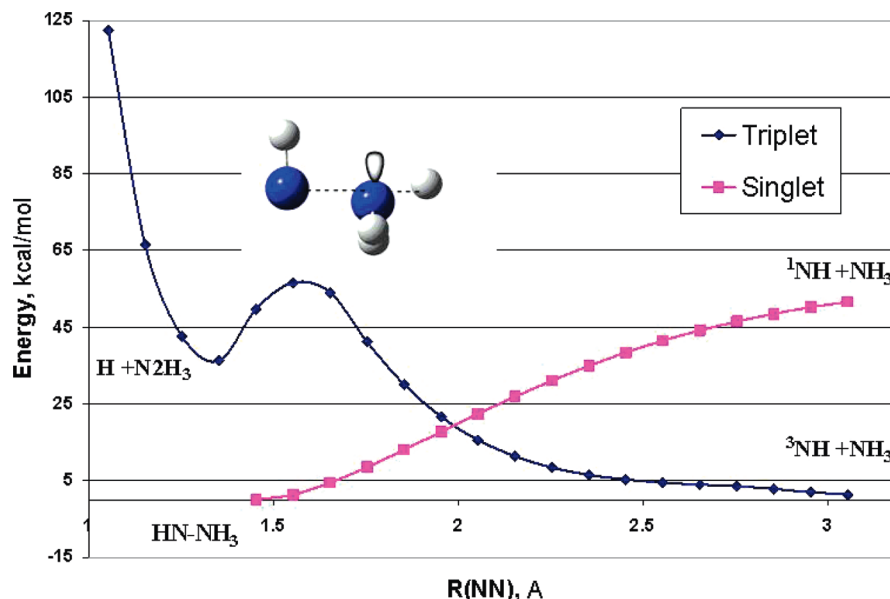
Figure 2. Minimal energy crossing point (MECP) between dissociation term of singlet NHNH$_3$ and Walden inversion reaction path of ammonia with triplet imidogen calculated at QCISD/6-311+G(2df,2p) level of theory (see text for further details).

the reader is referred to reviews on the thermochemistry of such particles.[6,55,65,66]

N−H Bond Dissociation in Hydrazine and its NH$_3$NH Isomer. The chain branching dissociation channel for hydrazine to N$_2$H$_3$ + H occurs at ~17 kcal mol^{-1} above the entrance level. Such process has an advantage in entropy and can play a certain role at higher temperatures (see kinetic section). The predicted dissociation limits are close to each other at different levels of theory. The product set is located 17.85, 17.5, and 16.1 kcal mol^{-1} higher than entrance channel at CCSD(T), QCISD(T) and CBS-QB3 levels, respectively (Table 2). Homolytic scission of the H−NH$_2$NH bond in iminoammonium ylide takes place at the 35.77, 35.80, and 38.9 kcal mol^{-1} dissociation limits at respective levels of theory.

Dissociation of N−H Bonds in Intermediate Radicals. Dissociation of N$_2$H$_3$ radical to the *trans-*, *cis-* and *iso-*N$_2$H$_2$ isomers occurs at 46.17, 51.3, and 69.53 kcal mol^{-1} correspondingly at the CBS-QB3 level.

Isomers of N$_2$H$_2$ and their Interconversion. Disproportionation reactions leading to the formation of diazene isomers are currently considered as the most relevant channels in hydrazine decomposition at low temperatures.[25,28] As mentioned above, N$_2$H$_2$ (the uncertain isomer) is registered mass-spectroscopically by Stothard[25] at room temperature, who set the reaction rate at 1.3 ± 0.5 × 10^{-12} cm^3 molecule^{-1} s^{-1} (~ 7.8 × 10^{11} cm^3 mol^{-1} s^{-1}). Nevertheless, unimolecular pathways to their formation are not apparent. Intertransition between diazene isomers could play a principal role in the overall reaction mechanism; however, these reactions are highly energetic processes as shown in numerous publications consonant with the results reported here. Barriers are rather high to become important, at least at lower temperatures.

Isomers of N$_2$H$_2$ (diazene or diimine) are studied extensively in the scientific literature and the isomerization of N$_2$H$_2$ is among the most studied theoretically, as a model reaction.[67] The geometry, relative energies, intertransition, and decomposition-recombination barriers of these species have been examined in detail at the variety of theoretical levels starting from earlier studies referenced by Jensen et al.,[68a] and Martin and Taylor[68b] ending with the recent calculations of Biczysco et al. at MRCI-Q level.[69] In this regard, we will discuss these topics here only

briefly considering just those pathways directly involved in the main transformation channels of N$_2$H$_4$.

The trans isomer of N$_2$H$_2$ is found to be the most stable structure and has been observed experimentally in contrast to the two other isomers. Theoretical results are consistent concerning the sequence of the stability of isomers (*trans-*N$_2$H$_2$, *cis-*N$_2$H$_2$, and NNH$_2$). The *cis-*N$_2$H$_2$ isomer is less stable than the trans isomer by 5.3, 5.4, and 5.6 kcal mol^{-1} at CCSD(T), QCISD(T) and CBS-QB3 levels, respectively, whereas the relative stability of NNH$_2$ with the same methods is 24.2, 21.9, and 23.3 kcal mol^{-1}.

There is agreement between methods on the prediction of significantly high barriers for isomerization. However, some methods failed to correctly predict details of all transition states. The main discrepancy between methods concerns the existence and the location of two *cis−trans* isomerization transition states (via either inversion of a nitrogen center or the rotation of imidogen groups about the N−N bond). The widely used MP2 method predicts the main features of the PES rather well, except the structure of the TS*t-t* transition state, which is claimed by Biczysco et al. to be unrealistic[69] Localized at the MP2 level this transition state is almost linear[30] while the authentic one at the MRCI-Q multireference level has an angular structure.[69]

The relative energies obtained in the present work are consonant with literature data (correspondingly via TS*iso*1 for *cis-*N$_2$H$_2$ to *trans-*N$_2$H$_2$ and TS*iso*2 for *trans-*N$_2$H$_2$ to *iso-*N$_2$H$_2$ *viz.,* a 1,2-hydrogen shift in the *trans-*N$_2$H$_2$ structure leading to the aminonitrene structure NNH$_2$, known also as *iso-*N$_2$H$_2$). For the sake of brevity in Figure 1 only the lower energy pathway via TS*iso*1 is presented to track only its relevance in the hydrazine decomposition process. CBS-QB3 geometries and energies again compare well with the experimental and literature theoretical calculations. TS*iso*2 is set to 27.2 kcal mol^{-1}, which is comparable to the energy of NH$_3$ + singlet NH product set.

3.6. Unimolecular Formation channels to trans-N$_2$H$_2$. *Reaction 10 via TS6 and Isomerization via TSiso1 and TSiso2.* As seen from the PES diagram, unimolecular formation of *trans-*N$_2$H$_2$ is a possible outcome because of the decomposition of NH$_3$NH (via TS6) and the isomerization of *cis-*N$_2$H$_2$ and NNH$_2$. The transition state for H$_2$-elimination, TS6, is located ca. 33 kcal mol^{-1} higher than the iminoammonium ylide intermediate
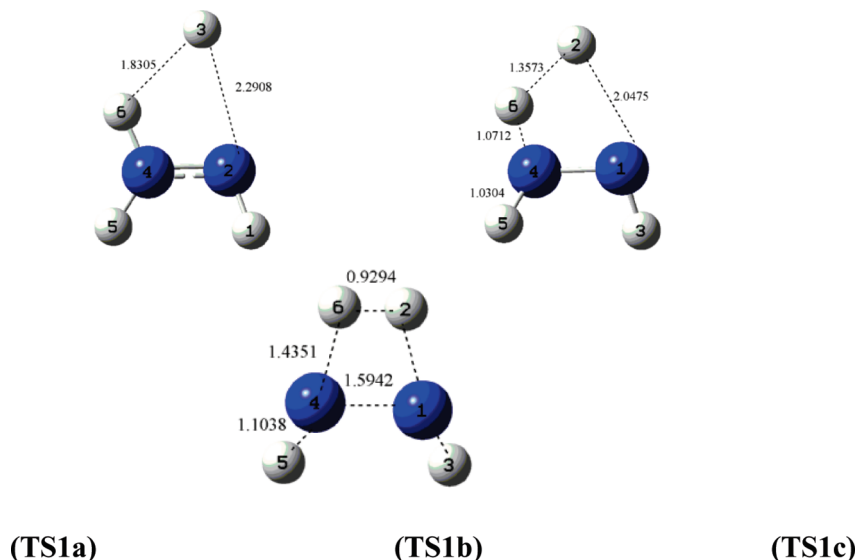
Figure 3. Different forms of the transition state TS1 for the $N_2H_4 \rightarrow N_2H_2$-*cis* + H_2 reaction, calculated at the CBS-QB3 (TS1a) and MP2/6-311+G(2df,2p) levels (TS1b and TS1c).

(see Table 2) and thus can perhaps be ruled out as a unimolecular source for the low temperature formation of H_2 and N_2H_2 observed experimentally by Stothard et al.[25] Isomerization from the cis isomer faces an even higher barrier of ca. 45 kcal mol^{-1} via TS*iso*1 versus 47 kcal mol^{-1} [61] and 44 kcal mol^{-1}.[30] The barrier for isomerization from NNH$_2$ (TS*iso*2, not shown in Figure 1 for simplicity) is ca. 48 kcal mol^{-1} vs literature values of 46 kcal mol^{-1},[61] and 46.5 kcal mol^{-1}.[30]

3.7. Unimolecular Formation of NNH$_2$. *Reaction 5* via TS4 and Isomerization via TS*iso*2. Formation of the aminonitrene structure NNH$_2$, suggested by Bozzelli and Dean[6] as the most relevant reaction channel (by fitting to experiment), is directly formed from activated and stabilized N_2H_4 via TS4. Nevertheless, this barrier is also significant. According to our calculations (Table 2), it is higher than the entrance channel by ca. $10-12$ kcal mol^{-1}. Thus, it also appears that this channel can be ruled out; it cannot be the most relevant channel for room temperature formation of hydrogen and N_2H_2 obtained experimentally.[25] This is reinforced by all theoretical methods predicting very similar structures for the transition state.

Formation of NNH$_2$ is also likely not possible via isomerization of *cis*-N_2H_2 because it requires overcome of a barrier of ca. 70 kcal mol^{-1}. Thus, unimolecular formation of *iso*-diazene at low temperatures also is not significant, but it can be formed through bimolecular reactions.

3.8. Unimolecular Channels to the Formation of cis-N$_2$H$_2$. *Reaction 4* via TS1, Reaction 11 via TS7, and Isomerization via TS*iso*1. The *trans*-N_2H_2 is the more stable isomer of diazene with an enthalpy of 48.5 kcal mol^{-1}, and it is observed experimentally. The cis-isomer is higher in energy by around 5.5 kcal mol^{-1}, and there is little in the way of an experimental assignment for this conformer.

The barrier for isomerization of *trans*- to *cis*-N_2H_2 is ca. 50 kcal mol^{-1} (52 kcal mol^{-1},[61] 50 kcal mol^{-1},[62] and 48.8 kcal mol^{-1}).[30] The reverse reaction barrier is also high as mentioned above, but somewhat lower because of the small exothermicity.

As seen from the potential energy diagram (Figure 1), the *cis*-N_2H_2 isomer appears to be extensively involved in several transformation channels. Theory predicts that it can be formed from decay of NH$_3$NH (via TS7). Decomposition of an activated intermediate occurs after surpassing a barrier of 34 kcal mol^{-1}; meanwhile the barrier relative to the entrance channel is some

12 kcal mol^{-1}. Again, all computational methods are in agreement, within a couple of kcal mol^{-1} (Table 2). Therefore, this channel can also be ruled out and will only be of significance at relatively high temperatures.

The isomerization barrier from *trans*-N_2H_2 to the cis- isomer is also too high to make this an important process. Despite the low endothermicity (5 kcal mol^{-1}) this reaction faces a barrier of ca. 50 kcal mol^{-1}, in agreement with the literature data mentioned above.

Formation of *cis*-N_2H_2 from either N_2H_4 or its isomer NH$_3$NH remains as the last possible unimolecular process, which could explain the experimentally observed low-temperature formation of hydrogen and N_2H_2. The other diazene formation channels are ruled out in the above discussion where all our theoretical and literature results are in agreement in predicting substantial barriers (cf. Figure 1).

The most intriguing H$_2$-elimination reaction channel is the direct formation of *cis*-diimide from activated hydrazine via TS1a located at the CBS-QB3 level (Figures 3a and 1). This process is followed by a novel further self-catalytic reaction, forming the simple products $N_2 + H_2 + H_2$ (vide infra) .The CBS-QB3 method predicts a barrier that is lower than the entrance channel by 13.3 kcal mol^{-1}, which would make these products facile from NH$_2$ + NH$_2$. This is the key result from our study, as it provides the only possible mechanism for the formation of dissociated products in the NH$_2$ + NH$_2$ reaction at below the entrance channel energy, with product formation potentially taking place at around the rate of association providing sufficiently high temperatures and/or low pressures. Alternatively, intersystem crossing to NH$_3$ plus triplet NH provides a forward reaction pathway to dissociated products proceeding at around the entrance channel energy, this could account for a majority of the [N_2H_4]* flux at higher temperatures.

The possibility of a low-energy reaction channel on the N_2H_4 PES could be a convenient path to the diimide + H$_2$ product set from stabilized hydrazine and from chemically activated [N_2H_4]* produced in the NH$_2$ + NH$_2$ reaction. This pathway could explain the experimental results of Stothard et al.,[25] who observed a source of diazene mass-spectroscopically at ambient temperatures (see also Kinetics section). The transition state proposed here more closely resembles one connected with the intermolecular H + N$_2$H$_3$ complex than N_2H_2 + H$_2$, as one can

see from Figure 3, although this still leads to H_2 elimination: $R(N_1-H_3) = 1.8$ Å, $R(N_2-H_3) = 2.04$ Å. Recalculation of the TS3a structure at the CCSD(T) level gives an even lower energy (-18.3 kcal mol^{-1}). However, this transition state remains questionable (vide infra).

According to the G2M(MP2) results of Hwang and Mebel,[30] the transition state from hydrazine to cis-N_2H_2 is extremely high; the barrier height is 150.1 kcal mol^{-1} above the energy of N_2H_4, placing it ca. 57 kcal mol^{-1} above the $2NH_2$ entrance channel. We have, therefore, studied the vicinity of this transition state in more detail. The relative energies obtained in this work are summarized in Figure 3. We have essentially localized four forms of TS1 within the same theoretical method (MP2). Two of these forms, along with the TS1 structure localized at the CBS-QB3 level, are depicted in Figure 3. We failed to find the identical transition state structure even within the moderate basis set MP2 method used by Mebel.[30] Instead, at the same MP2 level employing the larger 6-311++G(3df,3dp) basis set, we have managed to localize 3 other transition states in the vicinity of TS1 with vibrational modes leading to the same cis-N_2H_2 + H_2 products! One of these structures (not presented in Figure 3) has a loose structure resembling a van der Waals complex between a H atom and N_2H_3, with $R(H-H) = 3.3003$ Å, and is a roaming radical transition state. The reaction coordinate mode corresponds to the low frequency vibration ($\nu_1 = -29$ cm^{-1}). This barrier is higher than the entrance channel by ca. 30 kcal mol^{-1}, while the dissociation limit to H + N_2H_3 is less than 20 kcal mol^{-1}.

Another transition state, denoted as TS1b in Figure 3b, has a structure close to the CBS-QB3 geometry with more reasonable structural parameters of $R(H-N) = 1.35$ Å, $R(H-N) = 2.04$ Å. This transition state structure was located using restricted MP2 wave functions, and IRC analysis clearly indicates that it leads to formation of the proper reactants and products, with a sharp transition state topology ($\nu_1 = -1219.3$ cm^{-1}). Nevertheless, this channel is even higher in energy than the previous one ($\Delta^{\ddagger}H = 45$ kcal mol^{-1}). At the UMP2 level an almost identical transition state has been localized with a lower imaginary vibrational frequency ($\nu_1 = -149$ cm^{-1}). This structure, however, is highly spin-contaminated, with $\langle S^2 \rangle \approx 1$.

The third transition state, TS1c (Figure 3c), is similar to that localized by Hwang and Mebel, but the N—N bond is elongated by 0.15 Å from the equilibrium distance of 1.40 Å ($R(N-N)_{CBS-QB3} = 1.59$ Å vs $R(N-N)_{MP2} = 1.40$ Å). As one would expect for a process initiating the near-splitting of the strong N—N bond, this barrier is even higher than those reported above. IRC analysis does, however, indicate the proper path for movement from the reactant to the product set of interest. The structure of the transition state found in ref 30 is also close to cis-N_2H_2, with elongated N—H bonds that are being cleaved (1.51 and 1.43 Å) and a shortened H—H (1.16 Å) bond being formed. However, the N—N bond here is elongated substantially.

In light of the above-mentioned abundance of transition states at the MP2 level, the only version of TS1 predicted by CBS-QB3 (TS1a) also becomes questionable, and we identify that the electronic structure in the vicinity of these H_2 elimination transition states is truly complex. One needs to determine whether these four structures are real transition states leading to the elimination of H_2, and whether the formation of cis-N_2H_2 and H_2 via this channel is favored energetically; that is, whether or not TS1 is lower in energy than the NH_2 + NH_2 entrance channel.

The structure of TS1a predicted by the CBS-QB3 method is more representative of a N—H bond scission rather than H_2-

elimination ($R(H-H) = 1.83$ Å, $R(N-H) = 2.29$ Å). We have further studied this transition state structure with several higher-level methods. We note that optimization of the gradient norm for this structure at the MP2/6-311++G(3df,3dp) level resulted in the same TS1b structure predicted by the MP2 method with a moderate basis set, namely, shortening of the N_1-H_3 distance from 1.83 to 1.35 Å. Other methods, (W1 composite, B3LYP, MWKB1K, TPSSLYP1W density functional, and CCSD, MP2 ab initio methods) predict similar structures to that of CBS-QB3 for TS1 when calculations are initiated from the CBS-QB3 TS1 geometry. All these methods predict a structure for TS1, which is a van der Waals complex between H and N_2H_3 or a roaming radical transition state. The CBS-APNO search for TS1 leads to the TS4 structure (formation of NNH_2 + H_2), which probably results from the Hartree—Fock gradient norm optimization, in the calculation scheme of this multilevel method.

On the one hand, the CBS-QB3 result is more consistent, since it predicts only one TS1a and all our attempts to localize another transition state similar to TS1a and/or TS1b were unsuccessful. Single point recalculation of this structure at the CCSD(T)/6-311+(2df,2dp) level shows that the energy of this structure is indeed lower than the energy of the entrance channel, it is even lower than that predicted by CBS-QB3 (-18.3 vs -13.3 kcal mol^{-1}). However, the structure is not the first order TS at this particular level, but the superposition of four processes: two rotations, a bimolecular H + N_2H_3 and a unimolecular H_2 + N_2H_2. The T1 diagnostic test shows that this structure has considerable multireference character, much more than all the other studied transition states (0.182 vs 0.008–0.010).

It is worth remembering that CBS-QB3 geometries and energies compare well with the experimental and literature theoretical calculations on the energetics of isolated species (Thermochemistry section). CBS-QB3 is based on a structure localized using the B3LYP DFT functional, with 6-311(2d,d,p) basis set. The advantage of the CBS-QB3 method is that it includes additional corrections for spin-contaminated systems controlled by $\langle S^2 \rangle$. One main conclusion is that the direct elimination of H_2 is a highly energetic process. One can speculate about a lower-energy option as a consecutive process including near scission of an N—H bond, with further stripping (grabbing) of another hydrogen atom followed by the elimination of H_2. Such a process is relevant to the predictions of CBS-QB3.

Optimization of the gradient norm at the W1 composite level starting from the CBS-QB3 geometry again leads to the same TS1a structure predicted by CBS-QB3 with the calculated enthalpy even lower at -26.62 kcal mol^{-1}. We emphasize that while the multilevel W1 method employs DFT calculations for geometry optimization (though with a larger basis set than CBS-QB3), it uses a carefully selected set of higher level energy calculations.

Cis-diazene can be formed via bimolecular reactions, such as decomposition of $N_2H_3 \rightarrow$ cis-N_2H_2 + H (BDE at CBS-QB3 level is ca. 50 kcal mol^{-1}). Interaction of N_2H and H, as well as the recombination of two NH radicals can also occur but both these reactions would require high pressure to achieve collisional stabilization of the adducts. The energy gain from NH + NH is ca. 120 kcal mol^{-1} based on our CBS-QB3 enthalpy; $\Delta_f H^\circ_{298}$ (^{3}NH) = 86 kcal mol^{-1} and $\Delta_f H^\circ_{298}$ (cis-N_2H_2) = 53 kcal mol^{-1}.

TABLE 3: Rate Coefficients for Some of Elementary Reactions Involved in the N_2H_4 System (Input Parameters for QRRK/ME Analysis), $k = AT^n \exp(-E_a/RT)^a$

	reaction		A	n	E_a
1	$NH_2 + NH_2 = N_2H_4$	association	3.12×10^{13}	0.0	0.0
2	$NH_2NH_2 = NH_3NH$	Isom-TS3	1.3416×10^{11}	0.8555	6.4479×10^4
		reverse	5.3881×10^{11}	0.80279	2.000×10^4
3	$NH_2NH_2 = NNH_2 + H_2$	TS4	5.3779×10^9	1.2551	7.5322×10^4
4	$NH_2NH_2 = N_2H_2\text{-}cis + H_2$	TS1(low)	8.70×10^{12}	0.0	5.29×10^4
		TS1(high)	8.70×10^{12}	0.0	9.29×10^4
5	$NH_3NH = NH_3 + NH$	MECP	1.1032×10^9	1.6419	2.07×10^4
6	$NH_3NH = N_2H_2\text{-}trans + H_2$	TS6	5.7519×10^{10}	1.009	3.3753×10^4
7	$NH_3NH = N_2H_2\text{-}cis + H_2$	TS7	5.7519×10^{10}	1.009	3.4253×10^4
8	$NH_3NH = N_2H_3 + H$	dissociation	3.37×10^2	2.8178	2.2444×10^3
9	$N_2H_2\text{-}cis + H_2 = N_2 + H_2 + H_2$	TS2	3.2207×10^6	1.7991	2.144×10^4
10	$NH_2 + NH_2 = N_2H_2\text{-}trans + H_2$	TSc1t	8.7197×10^{10}	0.74673	8.345×10^3
11	$NH_2 + NH_2 = N_2H_2\text{-}cis + H_2$	TSc2t	1.6937×10^7	1.85255	1.0312×10^4
12	$NH_2 + NH_2 = NNH_2 + H_2$	TSc3t	4.1451×10^7	1.74352	3.948×10^3
13	$NH_2 + NH_2 = NH_3 + NH$	TSc5t	3.3717×10^7	2.81781	2.2444×10^3

^{a} Units: sec^{-1} or cm^3 mole^{-1} s^{-1}; E_a in cal mol^{-1}

4. Reaction Kinetics

4.1. Association Reaction $NH_2 + NH_2$. The association and subsequent collisional deactivation of amidogen radicals, reaction 1, is known as the principal channel for the NH_2 self-reaction at pressures higher than 100 mbar.[24]

$$NH_2 + NH_2(+M) \rightarrow N_2H_4(+M) \qquad (1)$$
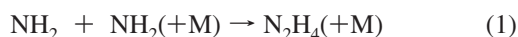
Early experimental studies of this reaction were discussed by Lesclaux and co-workers.[9] Photolysis of NH_3 or formamide gives $(4.7 \pm 2.0) \times 10^{13}$ cm^3 mol^{-1} s^{-1}.[14] The rate coefficient was evaluated by Lesclaux et al. at 4.2×10^{13} cm^3 mol^{-1} s^{-1}. The association rate constant evaluated by Sarkisov et al.[20] at 300 K using combined intracavity laser spectroscopy and flash photolysis of NH_3 is equal to 3.12×10^{13} cm^3 mol^{-1} s^{-1}, and has been used in previous modeling work by Dean and Bozzelli.[6] We employ the same value in our kinetic analysis as well.

According to Fagerström and co-workers,[26] termolecular stabilization is the dominant process at pressures in the range 200–1000 mbar of SF_6. The reaction was found to be strongly pressure dependent, and they claimed that at higher pressure (1000 mbar) at room temperature this reaction remains in the falloff regime. The rate constant for the association reaction of NH_2 radicals was found by Troe's analysis in the temperature range 200–400 K. We have analyzed the effect of increased association rates on the final processes using the higher value of 7.1×10^{13} cm^3 mol^{-1} s^{-1} suggested by Fagerström et al.

The $NH_2 + NH_2$ association reaction proceeds without any activation barrier.[55] Negative temperature dependence exists over the temperature range 293 K $\leq T \leq$ 501 K for the reaction of $NH + NH_3 \rightarrow$ products, indicating that the intermediate N_2H_4, which decomposes to $2NH_2$, is formed without a barrier.[57] However, at lower pressures the role of association is found to be minor (with He used as bath gas).[25] The reverse (dissociation) reaction rate constant is evaluated by Konnov at 5×10^{14} exp(-60.04 kcal mol$^{-1}/RT$) cm^3 mol^{-1} s^{-1}.[7]

4.2. QRRK/ME Kinetics Analysis. Elementary reaction rate constants calculated using transition state theory are listed in Table 3. Thermochemical parameters are presented in Table 4.
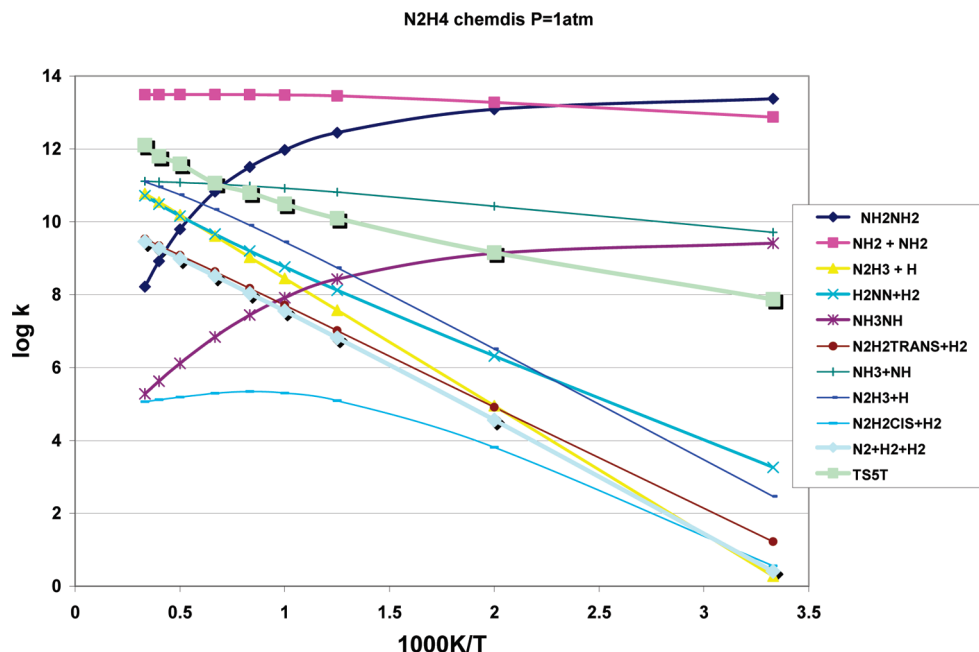

Figure 4. QRRK/ME kinetic analysis of chemical activation reaction of $NH_2 + NH_2$.

Kinetic Analysis of the NH₂ + NH₂ Reaction

J. Phys. Chem. A, Vol. 114, No. 21, 2010 **6245**

TABLE 4: Calculated Thermochemical Parameters[a]

SPECIES	$\Delta_f H^\circ_{298}$	S°_{298}	$C_p(300)$	$C_p(400)$	$C_p(500)$	$C_p(600)$	$C_p(800)$	$C_p(1000)$	$C_p(1500)$
H2	0	31.21	6.90	6.95	6.99	7.02	7.10	7.21	7.72
N2	0	45.77	6.96	6.99	7.07	7.2	7.51	7.82	8.32
3NH	86.28	43.29	6.97	6.96	6.99	7.05	7.23	7.46	8.04
NH1	127.0	41.67	6.98	7	7.11	7.27	7.61	7.91	8.43
NH2	45.04	47.9	8.02	8.2	8.45	8.74	9.38	10.04	11.39
NNH	59.57	53.63	8.32	8.83	9.36	9.88	10.85	11.52	12.44
NH3	−10.97	46.03	8.52	9.28	10.04	10.79	12.22	13.48	15.78
N2H2c	53.31	52.15	8.35	9.17	10.2	11.23	13.03	14.45	16.7
N2H2t	48.17	53.67	8.3	9.08	10.07	11.08	12.86	14.27	16.55
N2H2	48.17	53.67	8.3	9.08	10.07	11.08	12.86	14.27	16.55
NNH2	71.53	52.16	8.75	9.78	10.9	11.96	13.73	15.1	17.17
N2H3	54.1	56.69	10.42	12.04	13.52	14.79	16.82	18.42	21.19
N2H4	22.75	56.42	11	13.07	15.03	16.75	19.54	21.73	25.5
NH3NH	67.28	54.42	11.1	13.08	15	16.74	19.64	21.96	25.82
TS1	77.08	57.21	11.66	13.93	15.93	17.61	20.19	22.11	25.18
TS2	75.21	56.26	9.92	12.32	14.87	17.19	20.83	23.28	26.46
TS3	86.98	57.7	11.99	13.84	15.47	16.87	19.17	21.04	24.32
TS4	99.18	57	11.7	13.81	15.78	17.48	20.19	22.19	25.3
TS5T	93.18	63.43	13.9	15.84	17.47	18.81	20.92	22.55	25.31
TS6	100.98	56.39	11.14	13.42	15.46	17.16	19.8	21.76	24.93
TS7	101.48	56.39	11.14	13.42	15.46	17.16	19.8	21.76	24.93
MECP	88.08	56.39	13.9	15.84	17.47	18.81	20.92	22.55	25.31
TSC1T	113.7	61.18	13.4	15.16	16.59	17.72	19.4	20.62	22.63
TSC2T	116.67	59.98	12.5	14.97	17.15	18.94	21.57	23.38	26.07
TSC3T	110.2	60.18	12.7	14.99	17.02	18.71	21.24	23.01	25.72

[a] $S^\circ(T)$ and $C_p(T)$ in cal mol⁻¹ K⁻¹. Thermodynamic properties are referred to standard state of an ideal gas at 1 atm.

Figures 4 and 5 represent formation and decomposition features of chemically activated hydrazine derived from QRRK/ME analysis.

We estimate the effect of the lower limit rate for decomposition reaction of N₂H₄ via TS1 on overall processes by assuming the high barrier of activation (viz., ca. 30 kcal mol⁻¹ above entrance channel) for the formation of *cis*-N₂H₂ via TS1, as predicted by the MP2 method. As indicated above, all localized variants of TS1 at this level are above 30 kcal mol⁻¹, in accordance with the only related literature value calculated within the same method being even higher, 56.8 kcal mol⁻¹.[30]

In addition, QCISD(T)/6-311++(3df,2p) calculations on the geometry of CBS-QB3 as well as some other methods such as B97−1 also predict a higher energy for TS1. The calculated temperature dependence of rate constants for this system is depicted in Figure 5.

As seen from Figure 5, dominant processes at higher temperatures are the bimolecular disproportionation reaction leading to the formation of triplet imidogen and ammonia via TS5t (eq 6), as well as two simple decomposition reactions to the H + N₂H₃ product set, namely, reaction 1 generated from the stabilized N₂H₄ and reaction 13 produced from an activated

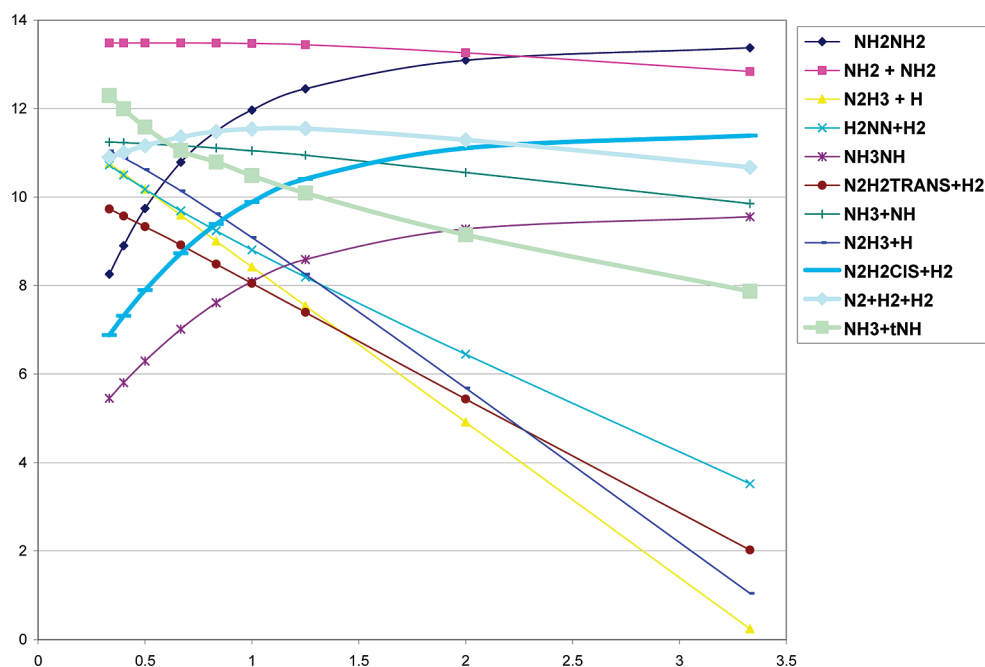**Figure 5.** QRRK/ME kinetic analysis of chemical activation reaction of NH₂ + NH₂ at $P = 1$ atm using high energy value for TS1 (see text for explanation).
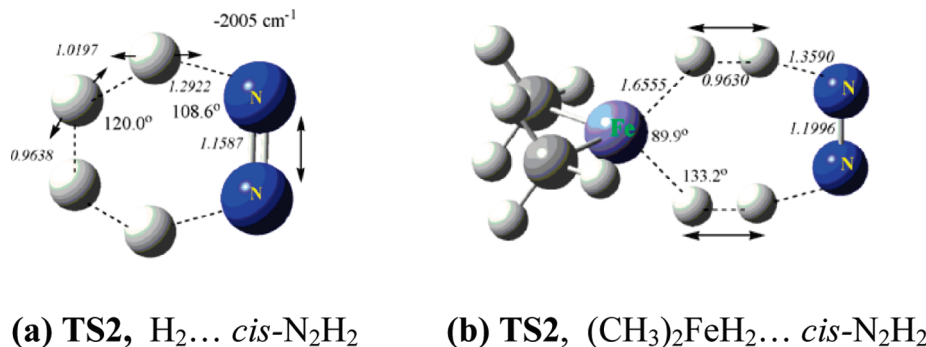
(a) TS2, $H_2 \ldots cis\text{-}N_2H_2$ **(b) TS2,** $(CH_3)_2FeH_2 \ldots cis\text{-}N_2H_2$

Figure 6. (a) Transition state for reaction 14: Gas-phase H_2-catalytic reaction: $N_2H_2\text{-}cis + H_2 = H_2 + H_2 + N_2$, (b) Transition state for reaction (14-3): metallocomplex model for H_2-elimination from the Fe-hydride: $(CH_3)_2FeH_2 + N_2H_2\text{-}cis = (CH_3)_2Fe + H_2 + H_2 + N_2$ (see text for further details).

intermediate NH_3NH. Kinetic analysis also predicts that $H + N_2H_3$ products can be formed an order of magnitude faster by this NH_3NH channel. Another dominant channel is the intersystem crossing reaction to the $^3NH + NH_3$ products.

On the other hand, W1 and CBS-QB3 methods as well as CCSD(T)/6-311++(3df,2p) method on the geometry of CBS-QB3 predict a barrier well below the entrance channel for TS1 (see Table 2 and Figure 1). In this regard, we have also performed kinetic analysis using also the low energy barrier for TS1 equal to -13 kcal mol^{-1}, as is predicted by the CBS-QB3 method (W1 and CCSD(T) values are much lower: at -26.6 and -18.3 kcal mol^{-1}, respectively).

As expected (Figure 4), the low energy form of TS1 results in formation of $cis\text{-}N_2H_2$ at even relatively low temperatures. This result, assuming that the localized transition state structure is not an artifact, could explain the experimental observation of diazene.[25] Accordingly, there is some experimental support for this uncertain product channel in the NH_2 self-reaction. Furthermore, the simple products N_2 and H_2 can be formed mainly from $cis\text{-}N_2H_2$. The dominant bimolecular disproportionation reactions are again the formation of triplet amidogen and ammonia via TS5t, as well as decomposition processes leading to the product set $H + N_2H_3$.

5. Dihydrogen Catalysis (Mediated by H_2-Decomposition of Diazene)

It is well-known that extreme conditions need to be applied to open the N_2 triple bond and to hydrogenate N_2. The role of hydrogen in the pyrolysis of ammonia and the decomposition of hydrazine is still controversial. In some early experiments[18] formation of simple product set $N_2 + H_2 + H_2$ is considered a priori as a possible channel in the decomposition of hydrazine. To our knowledge, there is no additional information on this. It is established only[16] that the addition of hydrogen substantially accelerates NH_3 removal in the pyrolysis of ammonia. Accordingly, one can also expect a specific role of hydrogen relevant to the formation and decomposition of activated hydrazine as well. Here we explore some new potential pathways including H_2 addition and elimination processes.

We have localized a new transition state (TS2, Figure 1 and Figure 6a) leading to the feasible formation of N_2 and H_2 final products.

$$cis\text{-}N_2H_2 + H_2 \rightarrow N_2 + H_2 + H_2 \qquad (14)$$
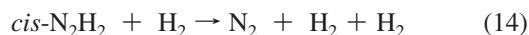
Stereoselective attack of a hydrogen molecule on the cis-isomer of N_2H_2 leads to a low barrier decomposition diazene via a six-

membered transition state ($\Delta^{\ddagger}H = 22.5$ kcal mol^{-1} at the CBS-QB3 and 24.8 kcal mol^{-1} at the CCSD(T) level). This process can be phenomenologically considered as "hydrogen molecule catalysis". The process is catalyzed by an extra hydrogen molecule (Figure 6a), and an extra H_2 is released as a product.

$$N_2H_2\text{-}cis + D_2 \rightarrow N_2 + 2DH \qquad (14\text{-}1)$$

In reality, the process is a pseudocatalytic one: in case of different hydrogen isotopic content of approaching hydrogen, for instance, produced hydrogen molecules will have mixed isotopic features.

Reverse termolecular reaction 14 leading to the gas-phase formation of $cis\text{-}N_2H_2 + H_2$ can be considered as a noncatalytic nitrogen fixation reaction with fairly low barrier of activation (77 kcal mol^{-1}). Importantly, this barrier is significantly lower than the current value for $N_2 + H_2$ bimolecular addition reaction (125 kcal mol^{-1} at G2M(MP2)//MP2/6-31G** level[30]). Termolecular reaction obviously is entropically less favorable but it may be a viable process at elevated pressures.

As the formation of cis-diazene is accompanied by the release of H_2 molecules (either via TS7 or TS1) the process can be considered as a self-sustaining one. Even more, the product set surpassing TS1 can be considered as a prereaction complex (mixture) facilitating further transformations.

A trimolecular channel is localized by Hwang and Mebel[30] involving NNH_2, however, with significantly higher barrier of activation than localized here TS2 for $cis\text{-}N_2H_2$ (101 kcal mol^{-1} vs 77 kcal mol^{-1}). CBS-QB3 predicts ca. 1 kcal mol^{-1} lower value for such a transition state (not shown for simplicity).

The N–N bond is extremely strong and hence N_2 reacts with H_2 in gas-phase only under extreme conditions, in presence of Fe-based catalysts. On the other hand, activation of nitrogen, its fixation, occurs in biological media supported by enzymes such as nitrogenase under much less severe conditions.[33,34] A termolecular reaction could easily take place supported by a transition metal containing stereoregulative biocatalyst, an enzyme. The conventional mechanism includes binding of N_2 to the $Fe[H]_2$ complex, reduction of N_2 to N_2H_2 and release of NH_3.[33]
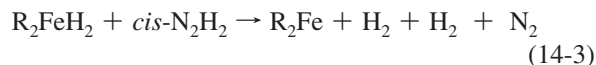
Importantly, hydrogen is always produced when nitrogenase reduces nitrogen to ammonia, and even high nitrogen pressures do not prevent evolution of hydrogen.[33] The ratio of hydrogen evolved to nitrogen fixed is close to 1:1, which implies that hydrogen evolution is obligatory in the fixation of molecular nitrogen by nitrogenase.

Kinetic Analysis of the NH$_2$ + NH$_2$ Reaction

J. Phys. Chem. A, Vol. 114, No. 21, 2010 **6247**

Hydrazine as an intermediate has been detected experimentally whereas N$_2$H$_2$ is assumed to be a very unstable intermediate that tends to decompose back to N$_2$ + H$_2$.[33]

The reaction 14 we revealed here could explain the evolution of hydrogen observed experimentally in biological media if one considers the supporting role of the stereoregulative catalysts.

In this regard, we have studied the negatively charged system (H$_2$ + *cis*-N$_2$H$_2$)$^-$ as well as metalorganic analogous to the reaction 14. The anionic system encounters the same type of barrier: somewhat lower at B3LYP level (15.50 kcal mol^{-1} vs 22.5 kcal mol^{-1} obtained for neutral system) and a bit higher at CBS-QB3 level (26.43 kcal mol^{-1}).

Intriguingly, exactly the same transition state (TS2) holds for the much more complex model reaction of (CH$_3$)$_2$FeH$_2$ with diazene, namely, when a hydrogen complex of a transition metal serves as a source of the "H$_2$-catalyst", an extra-H$_2$. This suggests that the mechanism is more general in nature. The process proceeds through the same transition state modes as the reaction 14 as shown in reaction (14-3) below and Figure 6.

$$R_2Fe + H_2 \leftrightarrow R_2FeH_2 \qquad (14\text{-}2)$$

$$R_2FeH_2 + cis\text{-}N_2H_2 \rightarrow R_2Fe + H_2 + H_2 + N_2 \qquad (14\text{-}3)$$

Calculations for this organometallic model system have been performed at B3LYP DFT level using the Dunning-Hay double-ζ basis set[72] and LanL (Los Alamos National Lab) pseudopotential for Fe[73] with the inner electrons substituted by the effective core potential to account for relativistic effects. The results obtained show that the transition state for the electrically neutral "heterogeneous" complex is much lower, 6 kcal mol^{-1} vs 22.5 kcal mol^{-1} for reaction 14. Hence, this process can take place in mild conditions.

The H-atom transfer process from the dimethyl Fe-hydride can be formally considered as a 2-electron transfer process, as the hydrogen atom in hydride is negatively charged and in diimide it is acidic in nature. Topologically, the same barrier holds also for the negatively charged "heterogeneous" system as it arise in case of "isolated" gas-phase reaction discussed above. The barrier for negatively charged transition metal containing complex is relatively higher.

A manifold of charges on transition metal central coordination-atoms (well presented in bioprocesses) could control dative metal−ligand interactions and the electron-acceptor interaction in a given complex and hence play a role of the regulator which switches between two possible options: formation and consumption of *cis*-N$_2$H$_2$, respectively, namely, leading to the enzymatic fixation of N$_2$. Detailed modeling is in progress.[35]

6. H + N$_2$H$_3$ Bimolecular Reactions

cis-N$_2$H$_2$ may serve as an important intermediate in metabolism of N$_2$H$_4$. It is therefore of value to identify other possible sources of *cis*-N$_2$H$_2$ formation. Apart from the discussed above unimolecular reaction via TS1, there is an option to its formation through bimolecular reactions involving, for example, the N$_2$H$_3$ radical. The bimolecular disproportionation reaction, H + N$_2$H$_3$ → H$_2$ + N$_2$H$_2$ is also one of the possible sources for formation of *cis*-N$_2$H$_2$ in combustion media. This reaction should not be an isomer specific one. The formation of *trans*-N$_2$H$_2$ is somewhat more favorable thermodynamically (by ca. 5 kcal mol^{-1}).

The important sources for its formation serve disproportionation reaction 2 as well as decomposition of the isomer of hydrazine, NH$_3$NH (eq 13). It is known also that N$_2$H$_3$ can be generated through photodissociation of N$_2$H$_4$, $k = 7 \times 10^{12}$ exp($-2500/RT$) at 222−657 K.[1d] The reported Arrhenius parameters are consistent with a metathesis reaction mechanism involving the abstraction of hydrogen from N$_2$H$_4$ by the H-atom.

The bimolecular hydrogen abstraction reaction in NH$_2$ + NH$_2$ leads also to the formation of NH$_3$ and triplet imidogen product set via TS5T, (eq 6). The same products are formed on the same triplet surface from the interaction of H + N$_2$H$_3$ via TS8t. This reaction involves exchange of NH by H, the Walden inversion via a local trigonal bipyramidal symmetry transition state (see, inserted structure in Figure 1).

Hydrogen Abstraction via Collinear Attack of H to N$_2$H$_3$ on Triplet Surface. We have localized transition states on the triplet surface for the collinear reactions of

$$H + N_2H_3 \rightarrow H_2 + trans\text{-}N_2H_2 \qquad (15)$$
$$\rightarrow H_2 + cis\text{-}N_2H_2$$
$$\rightarrow H_2 + iso\text{-}N_2H_2$$
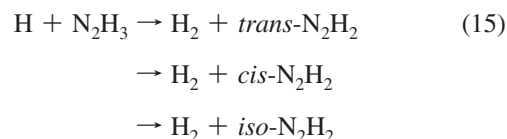
These reactions take place via transition states TSC1, TSC2, and TSC3. Thermochemical parameters for these transition states are presented in Table 4.

7. Conclusions

A detailed analysis of the literature data and a series of comprehensive theoretical calculations using a variety of high-level quantum chemical methods are presented to explain the mechanism of formation and decomposition of hydrazine mediated by chemical activation via recombination of two amidogen radicals.

Several of the pathways reported herein are unique and may play a principal role in the combustion of hydrazine and the pyrolysis of ammonia.

We suggest a novel mechanism for the formation of final products N$_2$ + H$_2$ + H$_2$ via unique phenomena "hydrogen molecule catalysis". The transition state structure in this hydrogen catalyzed reaction has a six-membered ring structure, and the process is strongly stereoselective. Feasible reaction parameters are predicted only in case of *cis*-N$_2$H$_2$ isomer of diazene. The activation barrier is fairly low, ca. 22.5 kcal mol^{-1} at CBS-QB3 and 24.8 kcal mol^{-1} at the CCSD(T)/CBS level.

Reverse termolecular reaction leading to the gas-phase formation of *cis*-N$_2$H$_2$ + H$_2$ can be considered as a noncatalytic nitrogen fixation reaction. The barrier calculated as of 77 kcal mol^{-1} is significantly lower than lowest value for bimolecular N$_2$ + H$_2$ addition reaction (125 kcal mol^{-1}).[30] The termolecular reaction is obviously unfeasible entropically. We show that stereoregulative transition-metal-containing catalysts such as hypothetical dimethyl iron hydride can facilitate decomposition of diazene, which could explain the obligatory evolution of hydrogen observed experimentally in the turnover cycle of nitrogenase.

6248 *J. Phys. Chem. A, Vol. 114, No. 21, 2010*

Asatryan et al.

References and Notes

(1) (a) Sutton, G. P. *Rocket Propulsion Elements. An Introduction to the Engineering of Rockets*; Wiley: New York, 1992. (b) Dagdigian, P. J. Transient Gas-phase Intermediates in the Decomposition of Energetic Materials, in *Overviews of Recent Research on Energetic Materials*; Shaw, R. W.; Brill, T. B.; Thompson, D. L. Eds.; World Scientific: Singapore, 2005; pp 129−160. (c) Adams, J. F.; Shaw, R. W., Jr. *Annu. Rev. Phys. Chem.* **1992**, *43*, 311−340. (d) Vaghjiani, G. L. *Int. J. Chem. Kinet.* **1995**, *27*, 777.

(2) (a) Gray, P.; Lee, J. C.; Spencer, M. *Combust. Flame* **1963**, *7*, 315. (b) Bunker, R. L.; Baker, D. L.; Lee, J. H. S. *Prog. Austronaut. Aeronaut.* **1991**, *133*, 325. (c) Pedley, M. D.; Bishop, C. V.; Benz, F. J.; Bennett, C. A.; McClenagan, R. D.; Fenton, D. L.; Knystautas, R.; Lee, J. H.; Peraldi, O.; Dupre, G.; Shepherd, J. E. *AIAA Prog. Austronaut. Aeronaut.* **1988**, *114*, 45. (d) Auzanneau, M.; Roux, M. *Combust. Sci. Technol.* **1990**, *73*, 505. (e) Kohlmann, J.-P.; Poppe, D. *J. Atmos. Chem.* **1999**, *32*, 397.

(3) Asatryan, R.; Bozzelli, J. W. *Self-Reactions of Amidogen (NH₂) Radicals and Decomposition of Chemically Activated Hydrazine*. Proceedings of the 6th US National Meeting on Combustion, Ann Arbor, MI, USA, May 2009.

(4) Benson, S. W. *Thermochemical Kinetics*; Wiley & Sons, Inc.: 1976; p 211.

(5) (a) Hanson, R. K.; Salimian, S. A kinetic study of nitric oxide removal from combustion gases by injection of NHi-containing compounds. In: *Combustion Chemistry*; Gardiner, W. C., Jr., Ed.; Springer-Verlag: New York, 1984. (b) Salimian, S.; Hanson, R. K. *Combust. Sci. Technol.* **1980**, *23*, 225.

(6) Dean, A. M.; Bozzelli, J. W. Combustion Chemistry of Nitrogen, In: *Gas-Phase Combustion Chemistry*; Gardiner, W. C., Jr., Ed.; Springer; New York, 1999; pp 125−341.

(7) Miller, J. A.; Bowman, C. T. *Prog. Energy Combust. Sci.* **1989**, *15*, 287.

(8) Konnov, A. A.; De Ruyck, J. *Combust. Flame* **2001**, *124*, 106.

(9) Lesclaux, R. *Rev. Chem. Intermed.* **1984**, *5*, 347−392.

(10) Dean, A. M.; Chou, M. S.; Stern, D. *Int. J. Chem. Kinet.* **1984**, *16*, 633.

(11) Diesen, R. W. *J. Chem. Phys.* **1963**, *39*, 2121.

(12) Salzman, J. D.; Bair, A. *J. Chem. Phys.* **1964**, *41*, 3654.

(13) Gordon, S.; Mulac, W.; Nangia, P. *J. Phys. Chem.* **1971**, *75*, 2087.

(14) Gehring, M.; Hoyermann, I. L.; Wagner, H.Gg.; Wolfrum, J. *Ber. Bunsenges. Phys. Chem.* **1971**, *75*, 1287.

(15) Back, R. A.; Yokota, T. *Int. J. Chem. Kinet* **1973**, *5*, 1039.

(16) Khe, P. V.; Soulignac, J. C.; Lesclaux, R. *J. Phys. Chem.* **1977**, *81*, 210.

(17) Pagsberg, P. B.; Eriksen, J.; Christensen, H. C. *J. Phys. Chem.* **1979**, *83*, 582.

(18) Dove, E. J.; Nip, W. S. *Can. J. Chem.* **1979**, *57*, 689.

(19) Lozovskii, V. A.; Nadtochenko, V. A.; Sarkisov, O. M.; Cheskis, S. G. *Kinetics Katal.* **1979**, *20*, 111.

(20) Sarkisov, O. M.; Cheskis, S. G.; Nadtochenko, V. A.; Sviridenkov, E. A.; Vedeneev, V. I. *Arch. Combust.* **1984**, *4*, 111.

(21) Patrick, R.; Golden, D. M. *J. Phys. Chem.* **1984**, *88*, 491.

(22) Dransfeld, P.; Hack, W.; Kurzke, H.; Temps, F.; Wagner, H. G. *Symp. Intern. Combustion Proc.* **1985**, *20*, 655.

(23) Cohen, N. *Int. J. Chem. Kinet.* **1987**, *19*, 319.

(24) Davidson, D. F.; Koshe-Hoinghaus, K.; Chang, A. Y.; Hanson, R. K. *Int. J. Chem. Kinet.* **1990**, *22*, 513−535.

(25) Stothard, N.; Humpfer, R.; Grotheer, H.-H. *Chem. Phys. Lett.* **1995**, *240*, 474.

(26) Fagerström, K.; Jodkowski, J. T.; Lund, A.; Ratajczak, E. *Chem. Phys. Lett.* **1995**, *236*, 103.

(27) Halat-Augier, C.; Dupre, G.; Paillard, C. E. *Shock Waves, Proc. Int. Symp., 20th* Sturtevant, B.; Shepherd, J. E.; Hornung, H. G. Eds.; Pasadena, Calif., 1995; Vol. 2, pp 893−898.

(28) Bahng, M.-K.; Macdonald, R. G. *J. Phys. Chem. A* **2008**, *112*, 13432.

(29) Xu, Z.-F.; Fang, D.-C.; Fu, X.-Y. *Int. J. Quantum Chem.* **1998**, *70*, 321.

(30) Hwang, D.-Y.; Mebel, A. M. *J. Phys. Chem.* **2003**, *107*, 2865−2874.

(31) Bespalov, V. Ya. *Zh. Obshchey Khim.* **1979**, *49*, 2620.

(32) (a) Fryzuk, M. D. *Acc. Chem. Res.* **2009**, *42*, 127−133. (b) Liu, Y.; Zhong, K.; Luo, K.; Gao, M.; Pan, H.; Wang, Q. *J. Am. Chem. Soc.* **2009**, *131*, 1862−1870. (c) Chen, P.; Xiong, Z.; Yang, L.; Wu, G.; Luo, W. *J. Phys. Chem. B* **2006**, *110*, 14221−14225.

(33) (a) Hoffman, B. M.; Dean, D. R.; Seefeldt, L. C. *Acc. Chem. Res.* **2009**, *42*, 609−619, and refs cited therein. (b) Holland, P. L. Nitrogen Fixation. In: *Comprehensive Coordination Chemistry II*; McCleverty, J., Meyer, T. J., Eds.; Elsevier:: Oxford, U.K., 2004; *Vol 8*, pp 569−599,and refs cited therein. (c) Hales, B. J.; True, A. E.; Hoffman, B. M. *J. Am. Chem. Soc.* **1989**, *111*, 8519−8520. (d) Howard, J. B.; Rees, D. C. *Proc. Nat. Acad. USA* **2006**, *103*, 17088. (e) Kim, J.; Rees, D. C. *Biochemistry*

1994, *33*, 389. (f) Howard, B.; Rees, D. C. *Chem. Rev.* **1996**, *96*, 2965. (g) Evans, D. J.; Henderson, R. A.; Smith, B. E. Catalysis by nitrogenase and synthetic analogs. In: *Bioinorganic Catalysis*; Redjik, J., Bouwman, E., Eds.; CRC Press: 1999; pp 153−209.

(34) (a) Volbeda, A.; Charon, M. H.; Piras, C.; Hatchikian, E. C.; Frey, M.; Fontecilla-Camps, J. C. *Nature* **1995**, *373*, 580. (b) Pavlov, M.; Siegbahn, P. E. M.; Blomberg, M. R. A.; Crabtree, R. H. *J. Am. Chem. Soc.* **1998**, *120*, 548−555.

(35) (a) Asatryan, R.; Bozzelli, J. W. *Dihydrogen Catalysis Phenomenon as an Option in Biological Fixation of N₂*; 238th ACS National Meeting, Washington, DC, USA, August, 2009. (b) Asatryan, R., Bozzelli, J. W. *Dihydrogen Mediated Hydrogen Transfer Reactions*; Fall Tech. Meeting, Eastern States Section, Combust. Institute, College Park, MD, USA, October, 2009.

(36) Miller, J. A.; Kee, R. J. Westbrook. *Annu. Rev. Phys. Chem.* **1990**, *41*, 345.

(37) (a) Baulch, D. L.; Bowman, C. T.; Cobos, C. J.; Cox, R. A.; Just, Th.; Kerr, J. A.; Pilling, M. J.; Stocker, D.; Troe, J.; Tsang, W.; Walker, R. W.; Warnatz, J. J. *Phys. Chem. Ref. Data*, *Vol. 34*, No. 3, 2005. (b) Vandooren, J.; Sarkisov, O. M.; Balakhnin, V. P.; Van Tiggelen, P. J. *Chem. Phys. Lett.* **1991**, *184*, 294. (c) Jodkowski, J. T.; Ratajczak, E.; Fagerström, K.; Lund, A.; Stothard, N. D.; Humpfer, R.; Grotheer, H.-H. *Chem. Phys. Lett.* **1995**, *240*, 63. (d) Dubinskii, I. V.; Lozovskii, V. A.; Sarkisov, O. M.; Khabarov, V. N.; Bulatov, V. P.; Buloyan, A. A. *Khim. Fizika* **1992**, *11*, 50. (e) K. Bulatov, V. P.; Ioffe, A. A.; Lozovskii, V. A.; Sarkisov, O. M. *Khim. Fiz.* **1990**, *9*, 1368−1374. (f) Song, S.; Hanson, R. K.; Bowman, C. T.; Golden, D. M. *Int. J. Chem. Kinet.* **2001**, *33*, 715−721. (g) Stephens, J. W.; Morter, C. L.; Farhat, S. K.; Glass, G. P.; Curl, R. F. *Chem. Phys. Lett.* **1993**, *97*, 8944. (h) Ioffe, A. A.; Bulatov, V. P.; Lozovskii, V. A.; Gol'denberg, M. Ya.; Sarkisov, O. M.; Umanskii, S. Ya. *Chem. Phys. Lett.* **1989**, *156*, 425.

(38) Dirtu, D.; Humelnicu, I.; Odochian, L. *Chimie* **2005**, *13*, 19.

(39) MacLean, D. I.; Wagner, H. Gg *Proc. Comb. Inst.* **1967**, *11*, 871.

(40) Michael, K. W.; Wagner, H. Gg *Proc. Comb. Inst.* **1965**, *10*, 353.

(41) Adams, G. K.; Stock, J. W. *Proc. Comb. Inst.* **1953**, *4*, 239.

(42) Frisch, M. J.; Trucks, G. W.; Schlegel, H. B.; Scuseria, G. E.; Robb, M. A.; Cheeseman, J. R.; Montgomery, Jr., J. A.; Vreven, T.; Kudin, K. N.; Burant, J. C.; Millam, J. M.; Iyengar, S. S.; Tomasi, J.; Barone, V.; Mennucci, B.; Cossi, M.; Scalmani, G.; Rega, N.; Petersson, G. A.; Nakatsuji, H.; Hada, M.; Ehara, M.; Toyota, K.; Fukuda, R.; Hasegawa, J.; Ishida, M.; Nakajima, T.; Honda, Y.; Kitao, O.; Nakai, H.; Klene, M.; Li, X.; Knox, J. E.; Hratchian, H. P.; Cross, J. B.; Adamo, C.; Jaramillo, J.; Gomperts, R.; Stratmann, R. E.; Yazyev, O.; Austin, A. J.; Cammi, R.; Pomelli, C.; Ochterski, J. W.; Ayala, P. Y.; Morokuma, K.; Voth, G. A.; Salvador, P.; Dannenberg, J. J.; Zakrzewski, V. G.; Dapprich, S.; Daniels, A. D.; Strain, M. C.; Farkas, O.; Malick, D. K.; Rabuck, A. D.; Raghavachari, K.; Foresman, J. B.; Ortiz, J. V.; Cui, Q.; Baboul, A. G.; Clifford, S.; Cioslowski, J.; Stefanov, B. B.; Liu, G.; Liashenko, A.; Piskorz, P.; Komaromi, I.; Martin, R. L.; Fox, D. J.; Keith, T.; Al-Laham, M. A.; Peng, C. Y.; Nanayakkara, A.; Challacombe, M.; Gill, P. M. W.; Johnson, B.; Chen, W.; Wong, M. W.; Gonzalez, C.; and Pople, J. A. *Gaussian 03, Revision D.01*; Gaussian, Inc.: Wallingford CT, 2004.

(43) Werner, H.-J.; Knowles, P. J.; Amos, R. D.; Bernhardsson, A.; Berning, A.; Celani, A.; Cooper, D. L.; Deegan, M. J. O.; Dobbyn, A. J.; Eckert, F.; Hampel, C.; Knowles, P. J.; Korona, T.; Lindh, R.; Lloyd, A. W.; McNicholas, S. J.; Mandy, F. R.; Meyer, W.; Mura, M. E.; Nicklass, A.; Palmieri, P.; Pitzer, R.; Rauhut, G.; Schü tz, M.; Schumann, U.; Stoll, H.; Stone, A. J.; Tarroni, R.; Thorsteinsson, T. *MOLPRO, version 2002.1.*

(44) (a) Cramer, J. C., *Essentials of Computational Chemistry*, 2nd ed.; Wiley: UK, 2004. (b) Vandeputte, A. G.; Sabbe, M. K.; Reyniers, M.-F.; Speybroyeck, V. V.; Waroquier, M.; Marin, G. B. *J. Phys. Chem. A* **2007**, *111*, 11771. (c) Asatryan, R.; Bozzelli, J. W. *Phys. Chem. Chem. Phys.* **2008**, *10*, 1769−1780. (d) Asatryan, R.; Bozzelli, J. W. Chain Branching and Termination in Low Temperature Combustion of n-Alkanes: 2-Pentyl Radical + O₂, Isomerization and Addition of Second O₂, *J. Phys. Chem. A*, submitted.

(45) (a) Montgomery, J. A., Jr.; Frisch, M. J.; Ochterski, J. W.; Petersson, G. A. *J. Chem. Phys.* **1999**, *110*, 2822−2827. (b) Montgomery, J. A., Jr.; Ochterski, J. W.; Petersson, G. A. *J. Chem. Phys.* **1994**, *101*, 5900.

(46) Martin, J. M. L.; De Oliveira, G. *J. Chem. Phys.* **1999**, *111*, 1843.

(47) Asatryan, R.; Bozzelli, J. W.; Simmie, J. M. *J. Phys. Chem. A* **2008**, *112*, 3172−3185.

(48) (a) Asatryan, R.; Bozzelli, J. W.; Simmie, J. M. *Int. J. Chem. Kinet* **2007**, *39*, 378−398. (b) Asatryan, R.; da Silva, G.; Bozzelli, J. W. *Novel Aspects in the Unimolecular Decomposition of RDX Explosive.*: 20th Intern. Symp. on Gas-Kinetics, Manchester, UK, July 2008. (c) da Silva, G.; Bozzelli, J. W.; Asatryan, R. *J. Phys. Chem. A* **2009**, *113*, 8596−8606. (d) da Silva, G.; Moore, E. E.; Bozzelli, J. W. *J. Phys. Chem. A* **2006**, *110*, 13979−13988. (e) da Silva, G. *Chem. Phys. Lett.* **2009**, *474*, 13−17. (f) da Silva, G.; Bozzelli, J. W. *J. Org. Chem.* **2008**, *73*, 1343−1353. (g) da Silva, G.; Bozzelli, J. W. *J. Phys. Chem. C* **2007**, *111*, 5760−5765.

(49) Lee, T. J.; Taylor, P. R. *Int. J. Quant. Chem. Symp* **1989**, *23*, 199.

Kinetic Analysis of the NH$_2$ + NH$_2$ Reaction

J. Phys. Chem. A, Vol. 114, No. 21, 2010 **6249**

(50) Chang, A. Y.; Bozzelli, J. W.; Dean, A. M. *Z. Phys. Chem.* **2000**, *214*, 1533.

(51) (a) Sheng, C.; Chang, A. Y.; Dean, A. M.; Bozzelli, J. W. *J. Phys. Chem. A* **2002**, *106*, 7276. (b) Sheng, C. Ph.D. Dissertation, NJIT: 2002.

(52) Ritter, E.; Bozzelli, J. W. *Int. J. Chem. Kinetics* **1991**, *23*, 767.

(53) Ruscic, B.; Berkowitz, J. *J. Chem. Phys.* **1991**, *95*, 4378.

(54) Melius, C. *BAC-MP4 Heats of Formaon and Free Energies*; Sandia National Laboratory: April **1993**.

(55) Gutowski, K. E.; Rogers, R. D.; Dixon, D. A. *J. Phys. Chem. A* **2006**, *110*, 11890–11897.

(56) Kee, R. J.; Rupley, F. M.; Miller, J. A. *The Chemkin thermodynamic data base*. Sandia Report SAND87-8215, 1987, and 1991 update. Sandia National Laboratories, Livermore, CA.

(57) Adam, L.; Hack, W.; Olzmann, M. *Z. Phys. Chem.* **2005**, *219*, 197–211.

(58) Gurvich, L. V.; Veyts, I. V.; Alcock, C. B., *Thermodynamic Properties of Individual Substances*, Fourth ed.; Hemisphere Publishing Corp.: New York, 1991; Vol 2.

(59) (a) Dixon, D. A.; Feller, D.; Peterson, K. A. *J. Chem. Phys.* **2001**, *115*, 2576–2581. (b) Matus, M. H.; Arduengo, A. J., III; Dixon, D. A. *J. Phys. Chem. A* **2006**, *110*, 10116–10121.

(60) Deng, Y.; Dixon, J. B.; White, G. N. *J. Colloid Interface Sci.* **2003**, *257*, 208–227.

(61) (a) Pople, J. A.; Raghavachari, K.; Frish, M. J.; Binkley, J. S.; Schleyer, P. v. R. *J. Am. Chem. Soc.* **1983**, *105*, 6389–6398. (b) Pople, J. A.; Curtis, L. A. *J. Chem. Phys.* **1991**, *95*, 4385.

(62) Pamidighantam, V. S.; Lammertsma, K. *J. Am. Chem. Soc.* **1991**, *113*, 1899.

(63) Ding, F.; Zhang, L. *Int. J. Quantum Chem.* **1997**, *64*, 447–452.

(64) Skurski, P.; Gutowski, M.; Simons, J. *J. Phys. Chem. A* **1999**, *103*, 625.

(65) Anderson, W. R. *J. Phys. Chem.* **1989**, *93*, 530.

(66) Foner, S. N.; Hudson, R. L. *J. Chem. Phys.* **1978**, *68*, 3162–3168.

(67) (a) Winter, N. W.; Pitzer, R. M. *J. Chem. Phys.* **1975**, *62*, 1269. (b) Peri, E, M.; Buenker, R. J.; Peyerimhoff, S. D. *Can. J. Chem.* **1977**, *55*, 1533. (c) Parsons, C. A.; Dykstra, C. E. *J. Chem. Phys.* **1979**, *71*, 3025. (d)

Pasto, D. J.; Chipman, D. M. *Ibid.* **1979**, *101*, 2290. (e) Pasto, D. J. *J. Am. Chem. Soc.* **1979**, *101*, 6852. (f) DeFrees, D. J.; Levi, B. A.; Pollack, S. K.; Binkley, J. S.; Pople, J. A. *J. Am. Chem. Soc.* **1979**, *101*, 4085. (g) Pouchan, C.; Dargelos, A.; Chaillet, M. *J. Mol. Spectrosc.* **1979**, *76*, 118. (gg) Kemper, M. J. H.; Buck, H. M. *Can. J. Chem.* **1981**, *59*, 3044. (h) Casewit, C. J.; Goddard, W. A, III *J. Am. Chem. Soc.* **1980**, *102*, 4057. (i) Dykstra, C. E. *Annu. Rev. Phys. Chem.* **1981**, *32*, 25. (j) Hout, R. F., Jr.; Levi, B. A.; Hehre, W. J. *J. Comput. Chem.* **1982**, *3*, 234. (k) Pople, J. A.; Raghavachari, K.; Frisch, M. J.; Binkley, J. S.; Schleyer, P. v. R. *J. Am. Chem. Soc.* **1983**, *105*, 6389. (l) Brandemark, U.; Siegbahn, P. E. M. *Theor. Chim. Acta* **1984**, *6*, 6–217. (m) Ito, K.; Nagase, S. *Chem. Phys. Lett.* **1986**, *126*, 531. (n) Schmidt, M. W.; Gordon, M. S. *Inorg. Chem.* **1986**, *25*, 248. (o) Walch, S. P. *J. Chem. Phys.* **1989**, *91*, 389. (p) Whitelegg, D.; Woolley, R. G. *J. Mol. Struct. (THEOCHEM)* **1990**, *209*, 23. (q) Pople, J. A.; Curtis, L. A. *J. Chem. Phys.* **1991**, *95*, 4385–4388. (r) Andzelm, J.; Sosa, C.; Eades, R. A. *J. Phys. Chem.* **1993**, *97*, 4664. (s) Smith, B. *J. Phys. Chem.* **1993**, *97*, 10513. (t) Andzelm, J.; Baker, J.; Scheiner, A.; Wrinn, M. *Int. J. Quantum Chem.* **1995**, *56*, 733. (u) Martin, J. M. L.; Taylor, P. R. *Spectrochim. Acta A* **1997**, *53*, 1039.

(68) (a) Jensen, H. J. A.; Jorgensen, P.; Helgaker, T. *J. Am. Chem. Soc.* **1987**, *109*, 2895. (b) Martin, J. M. L.; Taylor, P. R. *Mol. Phys.* **1999**, *96*, 681.

(69) Biczysco, M.; Poveda, L. A.; Varandas, A. J. C. *Chem. Phys. Lett.* **2006**, *424*, 46–53.

(70) Cox, J. D.; Wagman, D. D.; Medvedev, V. A., *CODATA Key Values for Thermodynamics*; Hemisphere Pub. Corp.: New York, 1984; p 1.

(71) Chase, M. W., Jr., *NIST-JANAF Thermochemical Tables*, Fourth ed.; J. Phys. Chem. Ref. Data, Monograph 9, 1998; pp 1−1951.

(72) Dunning, T. H.; Hay, P. J., In *Modern Theoretical Chemistry*; Schaefer, H. F., III, Ed.; Plenum Press: New York, 1976; p 1.

(73) Hay, P. J.; Wadt, W. R. *J. Chem. Phys.* **1985**, *82* (270), 299, 284.

(74) Biehl, E.; Stuhl, F. *J. Chem. Phys.* **1994**, *100*, 141–145.

(75) Rinnenthal, J. L.; Gericke, K.-H. *J. Mol. Spectrosc.* **1999**, *198*, 115–122.